CNWRA 2006-02

CORROSION OF ALLOY 22 IN CONCENTRATED NITRATE AND CHLORIDE SALT ENVIRONMENTS AT ELEVATED TEMPERATURES— PROGRESS REPORT

Prepared for

U.S. Nuclear Regulatory Commission
Contract NRC–02–02–012

Prepared by

Center for Nuclear Waste Regulatory Analyses
San Antonio, Texas

April 2006

CNWRA 2006-02

CORROSION OF ALLOY 22 IN CONCENTRATED NITRATE AND CHLORIDE SALT ENVIRONMENTS AT ELEVATED TEMPERATURES— PROGRESS REPORT

Prepared for

U.S. Nuclear Regulatory Commission
Contract NRC–02–02–012

Prepared by

L. Yang

Center for Nuclear Waste Regulatory Analyses
San Antonio, Texas

April 2006

PREVIOUS REPORTS IN SERIES

Number	Name	Date Issued
CNWRA 91-004	A Review of Localized Corrosion of High-Level Nuclear Waste Container Materials—I	April 1991
CNWRA 91-008	Hydrogen Embrittlement of Candidate Container Materials	June 1991
CNWRA 92-021	A Review of Stress Corrosion Cracking of High-Level Nuclear Waste Container Materials—I	August 1992
CNWRA 93-003	Long-Term Stability of High-Level Nuclear Waste Container Materials: I—Thermal Stability of Alloy 825	February 1993
CNWRA 93-004	Experimental Investigations of Localized Corrosion of High-Level Nuclear Waste Container Materials	February 1993
CNWRA 93-006	Characteristics of Spent Nuclear Fuel and Cladding Relevant to High-Level Waste Source Term	May 1993
CNWRA 93-014	A Review of the Potential for Microbially Influenced Corrosion of High-Level Nuclear Waste Containers	June 1993
CNWRA 94-010	A Review of Degradation Modes of Alternate Container Designs and Materials	April 1994
CNWRA 94-028	Environmental Effects on Stress Corrosion Cracking of Type 316L Stainless Steel and Alloy 825 As High-Level Nuclear Waste Container Materials	October 1994
CNWRA 95-010	Experimental Investigations of Failure Processes of High-Level Radioactive Waste Container Materials	May 1995
CNWRA 95-020	Expert-Panel Review of the Integrated Waste Package Experiments Research Project	September 1995
CNWRA 96-004	Thermal Stability and Mechanical Properties of High-Level Radioactive Waste Container Materials: Assessment of Carbon and Low-Alloy Steels	May 1996
CNWRA 97-010	An Analysis of Galvanic Coupling Effects on the Performance of High-Level Nuclear Waste Container Materials	August 1997

PREVIOUS REPORTS IN SERIES (continued)

Number	Name	Date Issued
CNWRA 98-004	Effect of Galvanic Coupling Between Overpack Materials of High-Level Nuclear Waste Containers—Experimental and Modeling Results	March 1998
CNWRA 98-008	Effects of Environmental Factors on Container Life	July 1998
CNWRA 99-003	Assessment of Performance Issues Related to Alternate Engineered Barrier System Materials and Design Options	September 1999
CNWRA 99-004	Effects of Environmental Factors on the Aqueous Corrosion of High-Level Radioactive Waste Containers—Experimental Results and Models	September 1999
CNWRA 2000-06 Revision 1	Assessment of Methodologies to Confirm Container Performance Model Predictions	January 2001
CNWRA 2001-003	Effect of Environment on the Corrosion of Waste Package and Drip Shield Materials	September 2001
CNWRA 2002-01	Effect of In-Package Chemistry on the Degradation of Vitrified High-Level Radioactive Waste and Spent Nuclear Fuel Cladding	October 2001
CNWRA 2002-02	Evaluation of Analogs for the Performance Assessment of High-Level Waste Container Materials	March 2002
CNWRA 2003-01	Passive Dissolution of Container Materials—Modeling and Experiments	October 2002
CNWRA 2003-02	Stress Corrosion Cracking and Hydrogen Embrittlement of Container and Drip Shield Materials	October 2002
CNWRA 2003-05	Assessment of Mechanisms for Early Waste Package Failures	March 2003
CNWRA 2004-01	Effect of Fabrication Processes on Materials Stability—Characterization and Corrosion	October 2003
CNWRA 2004-02	Natural Analogs of High-Level Waste Container Materials—Experimental Evaluation of Josephinite	January 2004

PREVIOUS REPORTS IN SERIES (continued)

Number	Name	Date Issued
CNWRA 2004-03	The Effects of Fabrication Processes on the Mechanical Properties of Waste Packages—Progress Report	July 2004
CNWRA 2004-08	A Review Report on High Burnup Spent Nuclear Fuel—Disposal Issues	September 2004
CNWRA 2005-01	Microbially Influenced Corrosion Studies of Engineered Barrier System Materials	October 2004
CNWRA 2005-02 Revision 1	Passive and Localized Corrosion of Overpack Materials—Modeling and Experiments	November 2005
CNWRA 2005-03	Microstructural Analyses and Mechanical Properties of Alloy 22	March 2005
CNWRA 2006-001	Crevice Corrosion Penetration Rates of Alloy 22 in Chloride-Containing Waters—Progress Report	December 2005

CONTENTS

Section Page

PREVIOUS REPORTS IN SERIES ii
FIGURES vii
TABLES ix
ACKNOWLEDGMENTS xi
EXECUTIVE SUMMARY xiii

1 INTRODUCTION 1-1

1.1 Objectives 1-3
1.2 Scope and Organization of the Report 1-3

2 EXPERIMENT 2-1

2.1 Test Specimens and Weight Loss Measurements 2-1
2.2 Test Setup 2-1
2.3 Electrochemical Measurements 2-5

3 RESULTS AND DISCUSSIONS 3-1

3.1 Chemistry of $NaCl$-$NaNO_3$-KNO_3 Mixture at Elevated Temperatures 3-1
3.1.1 Vapor Phase Chemistry 3-1
3.1.2 Liquid Phase Chemistry 3-3
3.2 Corrosion Behavior of Alloy 22 Materials 3-5
3.2.1 Open-Circuit Potential 3-5
3.2.2 Potentiodynamic Polarization Behavior 3-6
3.2.3 Vapor Phase and Liquid Phase Exposure Tests 3-8
3.2.3.1 Corrosion of Alloy 22 in Vapor and Liquid Phases 3-8
3.2.3.2 Effect of Temperature on the General Corrosion Rate of Alloy 22 3-9
3.2.3.3 Effect of Crevice on Corrosion of Alloy 22 3-11
3.2.3.4 Effect of Welds on Corrosion of Alloy 22 3-11
3.2.3.5 Exposure Time Effect on the Corrosion Rate of Alloy 22 3-11
3.3 Comparison with DOE Work 3-11
3.3.1 Open-Circuit Potential 3-11
3.3.2 Weight Loss Measurements 3-14

4 SUMMARY, CONCLUSIONS, AND RECOMMENDATIONS 4-1

4.1 Chemistry of Nitrate-Chloride Mixtures 4-1
4.2 Electrochemical Behavior of Alloy 22 4-1
4.3 Corrosion Rate 4-1

CONTENTS (continued)

Section Page

5 FUTURE WORK 5-1

5.1 Dust Effect on Corrosion of Alloy 22 5-1
5.2 Verification of Preferential Decomposition of Nitrate 5-1
5.3 Passivity and Pitting Corrosion of Alloy 22 5-1

6 REFERENCES 6-1

FIGURES

Figure		Page
2-1	Schematic Diagrams for the Creviced Specimens Used in the Tests.	2-3
2-2	Typical Weight Losses of Four Test Specimens and Two Baseline Specimens As a Function of Number of Cleaning Cycles in an ASTM HCl Solution	2-4
2-3	Typical Glass Vessels Used in the Experiment	2-4
3-1	Measured pH As a Function of the Ratio of Principal Cations ($Na^+ + K^+$) to the Principal Anions ($NO_3^- + Cl^-$)	3-3
3-2	(a) Measured pH and (b) Molar Ratio of Nitrate to Chloride in the Condensate As a Function of Temperature	3-4
3-3	(a) pH and (b) Ratio of Nitrate-to-Chloride of the Condensate As a Function of the Sum of the Principal Anions ($NO_3^- + Cl^-$)	3-4
3-4	Ratio of Nitrate to Chloride As a Function of the Sum of Novolatile Cations ($Na^+ + K^+$) to the Sum of the Principal Anions ($NO_3^- + Cl^-$)	3-5
3-5	Open-Circuit Potentials of Alloy 22 Specimens in Concentrated $NaCl$-$NaNO_3$-KNO_3 Solutions at 160 °C [320 °F]	3-6
3-6	Comparison of the Oxidation-Reduction Potential Measured with a Platinum Electrode with the Open-Circuit Potential of Alloy 22 Specimens in Concentrated	3-7
3-7	Potentiodynamic Polarization Curves on Alloy 22 Electrodes in Concentrated $NaCl$-$NaNO_3$-KNO_3 Solution at 160 °C [320 °F]	3-7
3-8	Corrosion Rate Calculated from Weight Loss of Specimens in the Vapor Phase and Liquid Phase Exposure Tests	3-8
3-9	Corrosion of a Thermally Aged Alloy 22 Specimen in Liquid and Vapor Phases After Exposure at 160 °C [320 °F]	3-9
3-10	Corrosion of the Horizontal Surface of Alloy 22 Specimen in Vapor Phase After Exposure at 160 °C [320 °F]	3-10
3-11	Corrosion Rates of Uncreviced Specimens at Three Different Temperatures As Shown in Figure 3-8.	3-10
3-12	(a) Corrosion of a Partially Creviced Specimen, (b) Corrosion Near a Creviced Area and (c) Corrosion at the Interface Between a Creviced Area	3-12
3-13	Optical and Scanning Electron Microscope Pictures Showing the Corrosion of a Welded Specimen Near the Weld After Exposure at 160 °C [320 °F]	3-13
3-14	General Corrosion Rates As a Function of Exposure Time for the Data Shown in Figure 3-8.	3-13
3-15	Steady-State Open-Circuit Potentials Measured by DOE in Deaerated Solutions Against Saturated Silver-Silver Chloride Electrode.	3-15
3-16	Comparison Between the Corrosion Rates of Alloy 22 Specimens in Concentrated Nitrate-Chloride Salt Mixtures Measured by the DOE	3-16

TABLES

Table		Page
1-1	Soluble Constituents in the Wet Precipitation Samples Collected at Death Valley, California, in Recent Years	1-2
2-1	Specimens Used in the Experiment	2-2
2-2	Chemical Compositions of Specimens and Weld Fillers (wt%)	2-3
3-1	pH and Ionic Concentrations in the Water Collected From the Condenser	3-2
3-2	Analyzed Liquid Phase Composition of the Salt Mixture at Test Temperatures	3-5

ACKNOWLEDGMENTS

This report was prepared to document work performed by the Center for Nuclear Waste Regulatory Analyses (CNWRA) for the U.S. Nuclear Regulatory Commission (NRC) under Contract No. NRC–02–02–012. The activities reported here were performed on behalf of the NRC Office of Nuclear Material Safety and Safeguards, Division of High-Level Waste Repository Safety. This report is an independent product of CNWRA and does not necessarily reflect the view or regulatory position of NRC.

The authors would like to thank D.S. Dunn, Y.-M. Pan, R.T. Pabalan, G.A. Cragnolino, A. Csontos, T. Ahn, R. Codell, and B. Leslie for technical discussions and helpful suggestions, and S. Young and B. Derby for laboratory assistance. The authors acknowledge the technical review of X. He, the editorial review of E. Hanson, the programmatic review of B. Sagar, and the assistance of J. Gonzalez in preparing this report.

QUALITY OF DATA, ANALYSES, AND CODE DEVELOPMENT

DATA: All CNWRA-generated original data contained in this report meet quality assurance requirements described in the Geosciences and Engineering Division Quality Assurance Manual. Experimental data have been recorded in CNWRA scientific notebook numbers 533 and 737. Sources for other data should be consulted for determining the level of quality for those data.

ANALYSES AND CODES: No codes were used in the analyses contained in this report.

EXECUTIVE SUMMARY

The performance of the waste packages at the potential repository at Yucca Mountain, Nevada, is one of the factors for the safe disposal of high-level waste. The U.S. Department of Energy (DOE) possible waste package design may consist of an outer container made of Alloy 22, a highly corrosion-resistant nickel-chromium-molybdenum alloy, and an inner container made of Type 316 nuclear grade stainless steel. Under nominal-case repository conditions, corrosion of the outer container is expected to be the primary degradation process limiting the lifetime of the waste package.

During the preclosure period, which may last for 50 to 300 years, DOE plans to ventilate the drifts of the potential repository for at least part of the time. Atmospheric aerosols and dusts may be introduced to the drifts by the ventilation and lead to the accumulation of hygroscopic salts on the waste package surfaces. The hygroscopic salts on the waste package surfaces could sorb moisture from the atmosphere and form brine solutions when the relative humidity is near or above their deliquescence relative humidity and affect corrosion of the waste package materials. According to the data collected near the Yucca Mountain area, nitrates, chlorides, sodium, and potassium are among the main soluble and thermodynamically stable ionic constituents in the dusts. Because of the extremely high boiling point of the solution formed by the NaCl, $NaNO_3$, and KNO_3 salts {> 220 °C [428 °F] at ambient pressure}, it may form aqueous solutions on the waste package surfaces during the high-temperature period of the repository system after the closure of the drift. The presence of aqueous solution during the high-temperature period has important implications because the waste package materials might be more susceptible to localized corrosion or may have high general corrosion rates at these temperatures. However, the understanding of the corrosion behavior of Alloy 22 in the presence of the highly hygroscopic salts is rather limited under the potential Yucca Mountain repository conditions.

The objectives of the studies presented in this report are to (i) study the chemistry of the liquid formed by the nitrate-chloride salt mixtures and the vapor above the liquid, and (ii) investigate the localized and general corrosion behavior of Alloy 22 in the liquid and vapor environment in an ambient-pressure system that was not deaerated to simulate the potential Yucca Mountain drift conditions at elevated temperatures.

An equimolar NaCl-$NaNO_3$-KNO_3 mixture was used in the study at a temperature range from 130 to 180 °C [266 to 356 °F] at ambient pressure in a glass vessel that was vented to the open air to simulate the potential Yucca Mountain drift condition. Ideally, a salt mixture that is closest to all eutonic compositions at different temperatures of the study should be used for the test because the eutonic composition has the lowest deliquescence relative humidity and is in the liquid form over a wide range of temperatures. However, such eutonic compositions of the NaCl-$NaNO_3$-KNO_3 system at test temperatures are unknown. The equimolar system was chosen because its composition is likely to be close to the eutonic composition.

The pH and chemical compositions of the vapor phase in the glass vessel were evaluated using samples collected from a condenser at the exit of the vent. The pH of the vapor phase condensate was low, suggesting that the salt mixture containing only the monovalent alkaline metal nitrates and chlorides was not stable and it decomposed slowly to form acid gases. The chemical composition measurements of the condensate showed that nitric acid was the primary acidic component. The concentration ratio of the nitric acid to the hydrochloric acid was high.

The higher content of nitric acid compared to the hydrochloric acid in the vapor phase implies that in the deliquescent salt mixtures that may be deposited on the waste packages, nitrates in the solid or liquid form could decompose preferentially to chlorides during the thermal pulse soon after the closure of the drift. Thus, the ratio of nitrate-to-chloride in the solution on the waste package surfaces will decrease and the ability of inhibiting localized corrosion of Alloy 22 by the nitrates may be compromised.

The open-circuit potential of Alloy 22 is an important parameter for the evaluation of localized corrosion. The open-circuit potentials of Alloy 22 specimens with different metallurgical conditions (mill-annealed, welded plus solution annealed) were measured in an ambient pressure system that was not deaerated. The stabilized open-circuit potential for the Alloy 22 specimens was approximately 0.3 V_{SCE}. The DOE measured open-circuit potential for the Alloy 22 material in similar salt mixtures in deaerated systems at ambient pressure, which was approximately -0.395 V_{SCE}. If the difference between the thermal liquid junction potential in the DOE tests and in the present work is ignored, the open-circuit potential measured by the DOE in deaerated and closed system was more than 600 mV lower than the open-circuit potential obtained in the system that was not deaerated and more relevant to the repository conditions.

Electrochemical polarization behavior of Alloy 22 in the salt mixtures is also important for the evaluation of the corrosion of waste package materials. Potentiodynamic polarization behaviors of creviced and uncreviced Alloy 22 materials were conducted in the solution of nitrate and chloride salt mixtures at elevated temperatures. The polarization curves showed no signs of significant localized corrosion.

The corrosion rates of Alloy 22 were measured in both the vapor and liquid phases of the $NaCl$-$NaNO_3$-KNO_3 salt mixture in the temperature range between 150 and 180 °C [266 and 356 °F] at ambient pressure. No significant localized corrosion was observed and general corrosion was found to be the primary attack mode. Compared with the general corrosion rates of Alloy 22 specimens measured in a similar salt mixture by the DOE in closed autoclave systems, the corrosion rate from the present study was 10 to 50 times higher. This large difference was probably due to the fact that the partial pressure of oxygen in the closed pressurized autoclave system used in the DOE tests was much lower than that in the system used in the present work. As confirmed by the open-circuit potential measurements, the corrosion potentials in the system that was not deaerated were much higher than those measured in deaerated systems. The high corrosion potential in the system used in the present work was probably the cause of the high corrosion rate. In addition, the corrosion rates measured by the DOE were conducted in a 4-month duration using foil specimens, and the corrosion rates presented in this report were conducted between 32 and 80 days with mostly thermally aged specimens. It is not known how the foil specimens were treated in the DOE tests. The high corrosion rates measured in the present study may also be due to the exposure time and heat treatment effects because, in general, corrosion rate decreases with time and thermally aged specimens have lower resistance to corrosion than mill-annealed specimens. Because thermally aging of the specimens simulates welding on the Alloy 22 containers in terms of heat treatment effect, the corrosion rate measured from the thermally aged specimens may represent the upper bound for the corrosion rates of Alloy 22 waste package containers.

It should be mentioned that the high corrosion rates presented in this report were measured in the presence of a large amount of salts relative to the surface area of Alloy 22. Under the expected Yucca Mountain conditions, only a small amount of salt mixtures may be deposited on

the surfaces of the waste packages. In addition, the nitrate and chloride salt mixtures will be found mixed with a relatively large amount of insoluble dusts. The corrosion of Alloy 22 by the soluble salt mixture in the presence of a large amount of insoluble dusts is expected to be reduced because the capillarity of the dust may reduce the ability for the soluble salt to wet the waste package surface. Additional studies are planned to assess the effect of insoluble dusts on the corrosion of waste package materials.

The preferential decomposition of the nitrate to the chloride observed in the short-term test could have an important implication to the evaluation of the waste package performance. Additional experiments at temperatures up to 220 °C [428 °F] are underway to verify this observation.

1 INTRODUCTION

Alloy 22 is a nickel-chromium-molybdenum alloy (Ni-22Cr-13Mo-4Fe-3W) and is highly corrosion resistant in oxidizing environments (Agarwal and Herda, 1997). Because of its high resistance to corrosion, Alloy 22 has been selected as the material for the outer container in the possible waste package design (Anderson, et al., 2003). The waste packages are important components of the engineered barrier system. The performance of the engineered barrier system is important to protect the public from any undue radiological risk before and after permanent closure. The U.S. Nuclear Regulatory Commission (NRC) has published licensing requirements for disposal of high-level wastes at Yucca Mountain. According to 10 CFR Part 63, the engineered barrier system must be designed so that, working in combination with natural barriers, radiological exposures to the reasonably maximally exposed individual and release of radionuclides into the accessible environment are limited. Under nominal-case scenario, corrosion is considered to be the primary degradation process limiting the lifetime of the waste package (Bechtel SAIC Company, 2004a). Loss of containment will allow the release of radionuclides to the environment immediately surrounding the waste packages.

In support of the NRC prelicensing activities on topics important to the postclosure performance of the potential repository, the Center for Nuclear Waste Regulatory Analyses (CNWRA) is conducting an independent technical assessment of corrosion processes that may affect the integrity of the waste packages. The corrosion-related processes considered important to the degradation of the waste packages include dry-air oxidation, humid-air and uniform aqueous (general) corrosion, localized (pitting, crevice, and intergranular) corrosion, microbially influenced corrosion, stress corrosion cracking, and hydrogen embrittlement. Based on the available risk insights and the NRC ranking, the passivity of the oxide film on waste packages and the failure mode of waste packages have high-to-medium significance on waste isolation (NRC, 2004).

During the preclosure period, that is expected to last for 50 to 300 years, the drifts of the potential repository will be ventilated at least for part of the time. Atmospheric aerosols and dusts may be introduced to the drift by the ventilation and lead to accumulation of hygroscopic salts on the waste package surfaces (Craig, et al., 2004; Pabalan, et al., 2002). The hygroscopic salts on the waste package surfaces will sorb moisture from the atmosphere and form brine solutions on the waste packages when the relative humidity is near or above their deliquescence relative humidity and affect corrosion of waste package materials (Orme, et al., 2004; Yang, et al., 2003; Pabalan, et al., 2002). The soluble contents of aerosol and dust in a given area are directly related to the soluble constituents in the rainfall collected in that area. According to the National Atmospheric Deposition Program, sodium, potassium, nitrates, and chlorides are among the principal soluble cation and anion constituents in the wet precipitation samples collected at Death Valley, California in recent years (National Atmospheric Deposition Program, 2004) (see Table 1-1). In Table 1-1, the value of each constituent for the deposition amount in terms of kg/ha (kilogram/hectare) was computed based on the concentration of the constituent in the wet precipitation and the amount of rainfalls. Because of the closeness and the wind direction near Yucca Mountain, the atmospheric deposition collected at Death Valley, California may be considered representative of the atmospheric dusts at Yucca Mountain.

Table 1-1. Soluble Constituents in the Wet Precipitation Samples Collected at Death Valley, California, in Recent Years*								
	Concentration in Wet Precipitation							
Year	Mg^{2+}†	Ca^{2+}†	K^{+}†	Na^{+}†	NH_4^{+}†	NO_3^{-}†	Cl^{-}†	SO_4^{2-}†
mg/L‡								
2000	0.58	0.066	0.023	0.22	0.82	1.9	0.3	0.74
2001	0.18	0.019	0.022	0.097	0.69	1.51	0.15	0.53
2002	2.91	0.191	0.145	1.114	1.1	4.31	0.83	2.27
Average	1.223	0.092	0.063	0.477	0.870	2.573	0.427	1.180
mM								
2000	0.024	0.002	0.001	0.010	0.051	0.031	0.008	0.008
2001	0.007	0.000	0.001	0.004	0.043	0.024	0.004	0.006
2002	0.120	0.005	0.004	0.048	0.069	0.070	0.023	0.024
Average	0.050	0.002	0.002	0.021	0.054	0.042	0.012	0.012
Deposition From Wet Precipitation								
kg/ha‡								
Year	Mg^{2+}†	Ca^{2+}†	K^{+}†	Na^{+}†	NH_4^{+}†	NO_3^{-}†	Cl^{-}†	SO_4^{2-}†
2000	0.26	0.029	0.01	0.098	0.37	0.85	0.13	0.33
2001	0.11	0.011	0.013	0.058	0.41	0.9	0.09	0.32
2002	0.2	0.013	0.01	0.078	0.08	0.3	0.06	0.16
Average	0.190	0.018	0.011	0.078	0.287	0.683	0.093	0.270
mole/ha‡								
2000	10.700	0.725	0.256	4.261	23.125	13.710	3.667	3.434
2001	4.527	0.275	0.332	2.522	25.625	14.516	2.539	3.330
2002	8.230	0.325	0.256	3.391	5.000	4.839	1.693	1.665
Average	7.819	0.442	0.281	3.391	17.917	11.022	2.633	2.810

*Source: National Atmospheric Deposition Program (NRSP–3)/National Trends Network. 2004. <http:/nadp.sws.uiuc.edu> (May 17, 2004).
†Mg^{2+}—Magnesium, Ca^{2+}—Calcium, K^{+}—Potassium, Na^{+}—Sodium, NN_4^{+}—Ammonium, NO_3^{-}—Nitrate, Cl^{-}—Chloride, SO_4^{2-}—Sulphate.
‡1 kg = 2.216 lb; 1 lb = 4.54×10^5 mg, 1 oz = 0.02957 L.

Because of the hydroscopic nature of the $NaCl$-$NaNO_3$-KNO_3 salt mixtures, their boiling points are extremely high (Rard, 2004,) and may be higher than 220 °C [428 °F] at ambient pressure.[1] According to the recent U.S. Department of Energy (DOE) analysis, the maximum temperature at the waste package surface will be 203 °C [397 °F] (Bechtel SAIC Company, 2004b) after the closure of the drift. Hence, brine solution may be present during the thermal pulse period of the repository system shortly after the closure. The presence of brine solution during the thermal pulse period has important implications because many metals are more susceptible to localized corrosion or has higher general corrosion rates at higher temperatures. The stability of nitrate in the solution on the waste package surface is also important to inhibit localized corrosion. If the nitrates decompose preferentially to the chlorides, the ratio of nitrate-to-chloride in the solution may decrease and the ability of inhibiting localized corrosion of Alloy 22 by the nitrates (Bechtel SAIC Company, LLC, 2004a; Dunn, et al., 2004) may be compromised. Experimental data on the corrosion behavior of Alloy 22 in a system that is similar to the Yucca Mountain environment at these temperatures have not been reported. DOE has recently conducted experiments in the nitrate-chloride mixture on the corrosion of Alloy 22 at high temperatures in closed autoclave system (Orme, et al., 2004). The oxygen partial pressure in the closed autoclave system may be lower than that in the potential repository system.

1.1 Objectives

The objectives of the present studies are to (i) study the chemistry of the liquid formed by the $NaCl$-$NaNO_3$-KNO_3 mixture and the vapor above the liquid, and (ii) investigate the localized and general corrosion behavior of Alloy 22 materials in the liquid and vapor environment that contains the $NaCl$-$NaNO_3$-KNO_3 mixture under simulated Yucca Mountain drift environments at elevated temperatures.

1.2 Scope and Organization of the Report

The chemical compositions of vapor and liquid phases of the system equilibrated by an equimolar $NaCl$-$NaNO_3$-KNO_3 salt mixture were measured. The corrosion behaviors of Alloy 22 specimens were characterized based on the electrochemical polarization behavior in the liquid phase and weight loss measurements in both the vapor and the liquid phases.

Ideally, a salt mixture that is closest to all eutonic compositions at different temperatures of the study should be used for the test because the eutonic composition has the lowest deliquescence relative humidity and is in the liquid form over a wide range of temperatures. However, such eutonic compositions of the $NaCl$-$NaNO_3$-KNO_3 system at the test temperatures are unknown. The equimolar system was chosen because its composition is likely to be close to the eutonic composition. The temperature range in which the experiments were conducted was from 130 to 180 °C [266 to 356 °F]. Because recent measurements by the DOE had shown that the boiling temperature of the $NaCl$-$NaNO_3$-KNO_3 salt mixtures was higher than 220 °C [428 °F], additional tests are underway for temperatures close to 220 °C.

[1]Bryan, C. "Localized Corrosion Due to Dust Deliquescence on the Alloy 22 Waste Package Outer Barrier." Presentation at the Nuclear Waste Technical Review Board, November 8–9, 2005. Slide 9. Las Vegas, Nevada. 2005.

The report is organized into five chapters, including introduction as Chapter 1. The experimental details are given in Chapter 2. The results and discussions are given in Chapter 3. Chapter 4 provides the summary, conclusions, and recommendations. The future work is included in Chapter 5.

2 EXPERIMENT

2.1 Test Specimens and Weight Loss Measurements

Both creviced and uncreviced Alloy 22 coupons with different metallurgical conditions were used in the experiments. The different specimens and their metallurgical conditions and geometry are given in Table 2-1. The schematic diagram of the creviced specimens is given in Figure 2-1. The creviced specimen is a slight modification from those used by Dunn, et al. (2005). The chemical compositions of these specimens are given in Table 2-2. All specimens were polished to 600 grit before use.

The weight loss measurements were conducted according to the ASTM-recommended procedure (ASTM International, 2005) using the *Th. A. plate* (Table 2-1) specimens. The posttest specimens were first cleaned with soft brushes, and rinsed with water and acetone. Then the posttest specimens were, along with one or two baseline specimens (uncorroded fresh specimens), cleaned in an HCl solution {150 mL [5.1 oz] with 1.19 specific gravity diluted to 1,000 mL [34 oz]} for 5 cycles of 3-minute immersions in an ultrasonically agitated bath, and for 5 cycles of 15-second immersions in a 50 wt% HF solution. The specimens were weighed after cleaning with soft brush and rinsing with acetone and water after each of the cleaning cycles. Figure 2-2 shows a typical plot for the weight loss measurements using the *Th. A. plate* (Table 2-1) specimens, including two baseline specimens, as a function of the number of cleaning cycles. There was no significant weight loss for the baseline specimens even in the HF solution. Most of the weight losses plateaued after the third cycle of cleaning in the HCl solution. Therefore, the weight losses after the third cycle of cleaning in the HCl solution were used to calculate the corrosion rate according to Eq. (2-1)

$$CR = 8.76 \times 10^7 \times \frac{W}{ATD} \tag{2-1}$$

where

CR	—	corrosion rate (μm/yr)
W	—	weight loss (g)
A	—	surface area (cm^2)
T	—	time (hour)
D	—	density (g/cm^3)

2.2 Test Setup

Figure 2-3 shows the schematic diagram of a typical test vessel. Approximately 1,000 g [2.2 lb] of salt mixture containing an equimolar NaCl, $NaNO_3$ and KNO_3 was placed in the glass vessel. The vessel was heated to the test temperatures {130 to 180 °C [266 to 356 °F]}. A small amount of deionized water was added to the vessel so that approximately half of the salts dissolved and half of the salts remained in the solid form at the bottom or on the wall of the glass vessel. The composition of the dissolved solution was determined by the phase diagram of the three compound salt mixture at the test temperature. Because the system was kept at ambient pressure and vented to the open air, small amount of water {10 to 20 mL [0.34 to 0.68 oz]} was periodically added to the vessel so that the system would automatically evaporate

Table 2-1. Specimens Used in the Experiment					
Specimens Code	**Heat Treatment**	**Heat Number of Base Metal**	**Heat Number of Filler Metal**	**Geometry**	**Surface Area (cm^2) [in^2]**
Th. A. Plate	Thermally aged at 870 °C [1,598 °F] for 30 minutes	2277-1-3150	Not applicable	1.27 × 1.27 × 0.15 cm^3 [0.5 × 0.5 × 0.06 in^3]	3.99 [0.618]
M.A. Cylinder	Mill-annealed specimens	2277-3-3266	Not applicable	48.6 × 6.2 mm* [1.91 × 0.24 in]*†	5.13 [0.795]
Welded Plate	Welded specimens	2277-3-3292	WN 813	1.27 × 2.54 × 0.15 cm^3 [0.5 × 1.0 × 0.06 in^3]	7.60 [1.18]
Creviced, M.A.	Creviced, mill-annealed specimen	2277-3-3266	Not applicable	Figure 2-1	12.9 [2.00]
Creviced, welded plus solution annealed–20	Creviced, welded plus solution annealed at 1,125 °C [2,057 °F] for 20 minutes	2277-3-3292	WN 813	Figure 2-1	12.9 [2.00]
Creviced, welded plus solution annealed–240	Creviced, welded plus solution annealed at 1,125 °C [2,057 °F] for 4 hours	2277-3-3292	WN 813	Figure 2-1	12.9 [2.00]

*Height × diameter.
†24.1 mm [0.95 in] of the height was immersed in liquid.

off the excess water through the condenser and maintain the water vapor pressure close to ambient pressure in the vapor phase. No purging was performed so that the system contains air during the tests.

The water in the condenser shown in Figure 2-3 was, from time to time, drained into a sample bottle for pH measurements and chemical analyses. The anions were analyzed using the ion chromatography method, and the cations were analyzed using the inductive coupled plasmer method. The pH and chemical analysis results were used to evaluate the chemical stability of the salts and the potential production of acid gases in the vapor phase. Because the water collected in the condenser was dilute and held at room temperature, it was expected that most of the gases, as a result of the decomposition of the salts in the glass vessel, would be captured

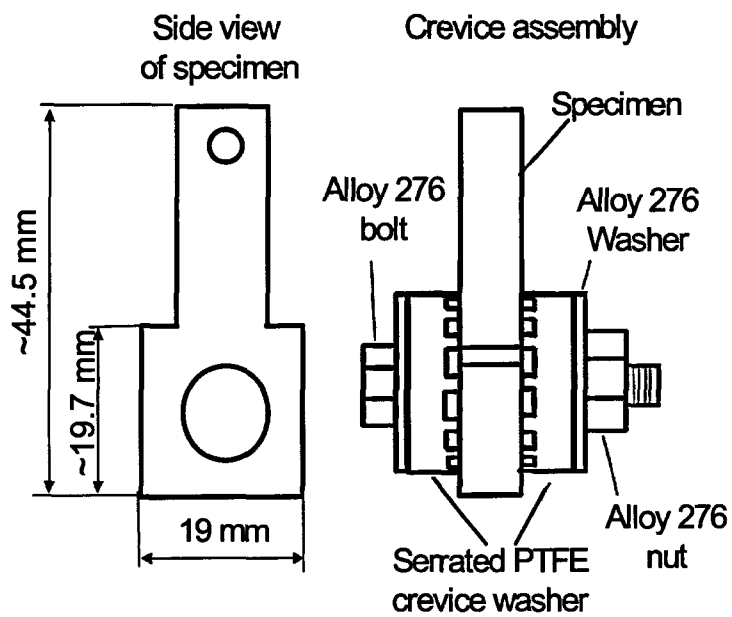

Figure 2-1. Schematic Diagrams for the Creviced Specimens Used in the Tests.
Note: PTFE—polytetrafluoroethlene; 1 in = 25.4 mm.

Table 2-2. Chemical Compositions of Specimens and Weld Fillers (wt%)

Heat Number	Ni*	Cr*	Co*	Fe*	Mo*	Mn*	W*	V*	Si*	C*	S*	P*
2277-1-3150	Bal†	21.1	1.70	4.5	13.2	3.5	2.9	0.16	0.03	0.003	0.004	0.008
2277-3-3266	Bal	21.4	1.19	3.75	13.30	0.23	2.81	0.14	0.03	0.005	0.004	0.008
2277-3-3292	Bal	21.22	1.32	3.69	13.64	0.23	2.96	0.13	0.02	0.004	0.003	0.005
WN813	Bal	22.24	0.41	2.37	13.7	0.34	3.13	0.01	0.02	0.003	0.001	0.003

*Ni–Nickel, Cr–Chromium, Co–Cobalt, Fe–Iron, Mo–Molybdenum, Mn–Manganese, W–Tungsten, Si–Silicon, C–Carbon, S–Sulfur, P–Phosphorus
†Bal—Balance

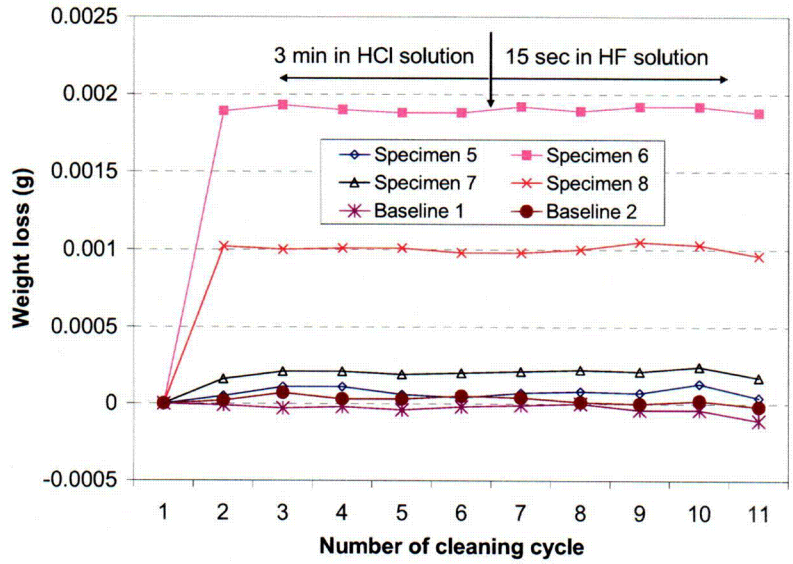

Figure 2-2. Typical Weight Losses of Four Test Specimens and Two Baseline Specimens As a Function of Number of Cleaning Cycles in an ASTM HCl Solution (ASTM International, 2005) and in 50 wt% HF Solution. The Weight Loss After the Third Cycle of Cleaning in the ASTM HCl Solution Was Used in the Weight Loss Analysis for Each Specimen. Note: 1 lb = 454 g.

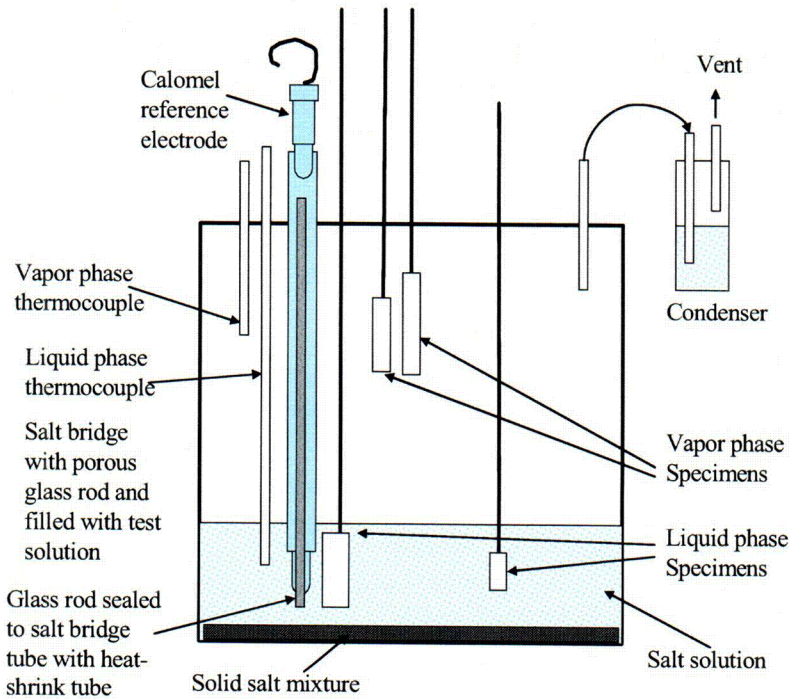

Figure 2-3. Typical Glass Vessels Used in the Experiment. The Total Volume of the Vessel is Approximately 3 L [102 oz].

C01

by the condenser. The condenser acted as a gas scrubber. Before the test and each time after the condenser was drained for sampling, a small amount of deionized water {15 mL [0.51 oz]} was added to the condenser to trap the gas entering the glass tube.

Samples of known volume and weight were taken from the liquid phase of one salt mixture at two elevated temperatures and analyzed for the equilibrium chemical compositions at these two temperatures. The samples were crystalized as soon as the temperature dropped. These solid samples were then diluted to 300 mL [10.14 oz] using deionized water before they were sent to the chemistry laboratory for analysis.

Test specimens were placed in the vapor phase and liquid phase of the vessel (Figure 2-3). The vessel was heated in a mantel and thermocouples were used to measure the temperatures of the liquid phase and vapor phase near the vapor phase specimens. Because of the thermal gradient from the bottom to the top of the vessel, the temperature at the vapor phase specimen location was usually 20 to 30 °C [36 to 54 °F] lower than that of the liquid temperature during normal testing. However, the temperature at the vapor phase specimen location could be approximately 30 to 40 °C [54 to 72 °F] higher than that of the liquid temperature during the evaporation of excess water because part of the evaporated water condensed on the surfaces at the top section of the vessel and dripped back to the bottom of the vessel. The condensed water was cooler than the vapor and lowered the temperature of the liquid phase when it dripped back to the bottom of the vessel. It was noticed that the temperature of the liquid phase was sometimes 20 to 25 °C [36 to 45 °F] lower and the temperature of the vapor phase was 20 to 25 °C [36 to 45 °F] higher than the set temperature during the evaporation of excess water in some of the tests.

2.3 Electrochemical Measurements

One of the test vessels was furnished with a salt bridge and a saturated calomel electrode for the measurements of the open-circuit potential and the potentiodynamic polarization behaviors. Even though reference electrodes are available for applications at temperatures up to 300 °C [572 °F] (Yang, 1999) under high pressure conditions, it is a challenge to construct a reference electrode that is usable at ambient pressure and at elevated temperatures. This is because the salt bridge is usually filled with a saturated KCl solution that boils at temperatures beyond 110 °C [230 °F] at ambient pressure (Brossia, et al., 2001). In this experiment, the high-boiling point test solution (equimolar $NaCl$-$NaNO_3$-KNO_3 mixture) was used to fill the salt bridge and a porous glass rod (Vycor by Dow Corning) was fitted inside the salt bridge from bottom to the top to maintain the electrical continuity in the presence of gas bubbles that were often formed inside the bridge because of boiling. The glass rod was sealed to the salt bridge at the bottom end by heat-shrink polytetrafluoroethylene tube. The thermal liquid junction potential in the salt bridge is not known. The analyses by Lvov and Macdonald (1996) indicated that the thermal liquid junction potentials for dilute chloride solutions were less than ± 50 mV from room temperature to 200 °C [392 °F]. Because the measurements of the open-circuit potential and polarization behavior were conducted with the same reference electrode, the absolute value may not be important for the purpose of this experiment. This thermal liquid junction potential can be calibrated with an external-pressure balanced reference electrode (Lvov and Macdonald, 1996) in an autoclave at a later time, should the need to know the precise absolute values of the measured open-circuit potentials and polarization behaviors during this study arise.

During a polarization test, the potential of the electrode was scanned from the open-circuit potential in the anodic direction. When the current reached 2×10^{-4} A, the electrode was held galvanostatically at 2×10^{-4} A for 2 hours. At the end of the 2 hours, the potential of the electrode was scanned in the cathodic direction until −0.2 to −0.4 V_{SCE}. The scan rate was 0.167 mV/sec. In cases where the current value of 2×10^{-4} A could not be reached when the potential was increased to 1.2 V_{SCE}, the galvanostatic step was ignored by the program to avoid excessive polarization.

3 RESULTS AND DISCUSSIONS

3.1 Chemistry of $NaCl$-$NaNO_3$-KNO_3 Mixture at Elevated Temperatures

It is well known that the chloride-nitrate salt mixture solution comprising of calcium or magnesium cations are unstable at temperatures near their boiling points. These salt mixtures decompose and produce acid gases (Pulvirenti, et al., 2003, 2004; Hailey and Gdowski, 2003). However, it is not known if the salt mixture solutions containing only monovalent alkaline metals decompose and, if they do, which of the salts (chlorides versus nitrates) would decompose first. It has been suggested that based on thermodynamic calculations, the degassing of the monovalent brines containing chloride and nitrate would increase the concentration ratio of nitrate to chloride in liquid phase.[1]

3.1.1 Vapor Phase Chemistry

Table 3-1 shows the pH and the concentrations of the ionic species of the water samples collected from the condenser (see Figure 2-3), which contained approximately 15 mL [0.51 oz] of initial water. The pH values varied from 1.9 to 4.3, which indicates that the salt mixtures containing only monovalent metals such as $NaCl$, $NaNO_3$, and KNO_3 were not stable and they decomposed to form acidic gases. Except for two samples, Cond-A-150 °C-06/17/05 and Cond-A-170 °C-06/16/05, that contained high concentrations of K^+ and Na^+, the ratio of NO_3^- to Cl^- varied between 2 and 59, indicating that the acid gases were mainly nitric acid, which suggests that nitrate salts decomposed preferentially to the chloride salts. It is interesting to note that many of the condenser water samples also contained high concentrations of K^+ and Na^+ or high ratio of K^+ and Na^+ concentrations to that of the total of the principal anions (Cl^- + NO_3^-). The high contents of the nonvolatile cations (K^+ and Na^+) are an indication that these condenser water samples were contaminated by liquid phase components which were carried out with the flow during evaporation. Figure 3-1 shows that the pH increased with the increase in the ratio of the sum of nonvolatile cations (K^+ + Na^+) to the sum of principal anions (Cl^- + NO_3^-), suggesting that the high pH (near 4) may not be representative of the vapor phase composition because of the contamination by the liquid phase composition.

Figure 3-2 appears to show that the pH increased with temperature and the ratio of nitrate to chloride in the vapor phase decreased with temperature in the range tested {130 to 180 °C [266 to 356 °F]}. A detailed examination indicates that the data points obtained near 180 °C [356 °F] contain high contents of nonvolatile cations (K^+ + Na^+) relative to the total of anions. Therefore, these data were more contaminated by the liquid phase composition. The important information from Figure 3-2 is that in the temperature range tested, the condensates were acidic and the concentration ratio of the nitrate to chloride was high.

Because it is difficult to control the evaporation rate, the samples in the condenser were collected whenever enough volume {10 to 20 mL [0.34 to 0.68 oz]} was accumulated, rather

[1]Bryan, C. "Localized Corrosion Due to Dust Deliquescence on the Alloy 22 Waste Package Outer Barrier." Presentation at the Nuclear Waste Technical Review Board, November 8–9, 2005. Slide 11. Las Vegas, Nevada. 2005.

Table 3-1. pH and Ionic Concentrations in the Water Collected From the Condenser								
Sample Identification	Temperature °C [°F]	pH	Cl^- (mM)	NO_3^- (mM)	K^+ (mM)	Na^+ (mM)	NO_3^-/Cl^-	$(K^+ + Na^+)/(Cl^- + NO_3^-)$
Cond-A-150°C-09/08/05	150 [302]	2.6	0.406	3.38	0.414	0.413	8.33	0.219
Cond-A-150°C-09/26/05	150 [302]	2.3	0.423	8.29	0.376	0.274	19.6	0.0747
Cond-A-150°C-10/17/05	150 [302]	2.5	0.783	4.61	0.760	0.268	5.88	0.191
Cond-A-150°C-06/17/05	150 [302]	3.2	1.77	0.561	1.68	0.622	0.316	0.987
Cond-A-160°C-06/13/05	160 [320]	4.2	0.227	1.29	0.440	0.578	5.66	0.673
Cond-A-170°C-06/16/05	170 [338]	3.1	1.46	1.54	1.60	0.496	1.06	0.699
Cond-B-130°C-09/26/05	130 [266]	2.1	0.403	14.6	0.335	0.238	36.2	0.0383
Cond-B-160°C-10/17/05	160 [320]	1.9	0.344	20.4	0.104	0.311	59.2	0.0200
Cond-C-170°C-09/13/05	170 [338]	3.5	0.358	0.736	0.338	0.220	2.06	0.508
Cond-C-170°C-09/07/05	170 [338]	3.2	0.111	1.11	0.0860	0.269	10.0	0.290
Cond-C-170°C-09/26/05	170 [338]	3.1	0.527	1.48	0.496	0.313	2.81	0.403
Cond-C-180°C-08/22/05	180 [350]	4.3	0.620	2.36	0.0839	0.817	3.80	0.303

than on regular time intervals. The relationship between the analyzed results as a function of the total anion concentrations provides a good indication of the evaporation time effects. Figure 3-3 shows that the pH decreased, and the ratio of NO_3^- to Cl^- increased with the increase of the total amount of the principal anions ($NO_3^- + Cl^-$). These trends suggest that the pH of the condensate may be even lower than 1.9 and the ratio of NO_3^- to Cl^- may be even higher than 59.2 for a longer evaporation time.

The high ratio of NO_3^- to Cl^- in the vapor phase suggests that the nitrates in the salt mixture decomposed more than the chlorides. This process may lead to the decrease, when the drift temperature is high, in the ratio of nitrate to chloride in the salt mixtures that may be deposited, during the ventilation period, on the waste package or drip shield surfaces. Therefore, the ability of inhibiting localized corrosion of Alloy 22 by the nitrate (Bechtel SAIC Company, LLC, 2004a; Dunn, et al., 2004) may be compromised during the postclosure period.

It should be mentioned that the decomposition rate was low because it took several days, even more than a week, for the condenser water {10 to 20 mL [0.34 to 0.68 oz]} to become acidic.

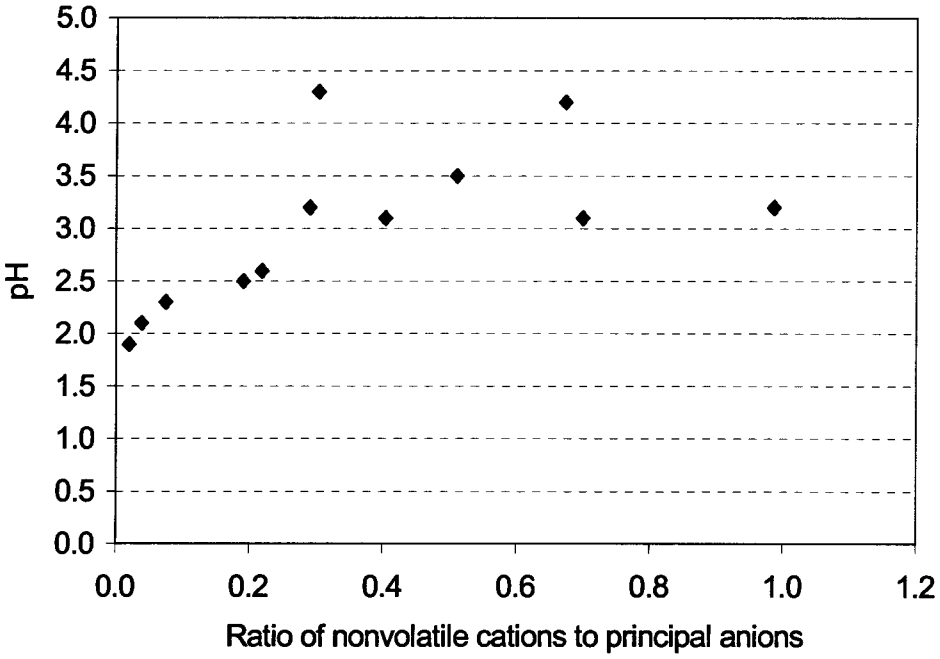

Figure 3-1. Measured pH As a Function of the Ratio of Principal Cations ($Na^+ + K^+$) to the Principal Anions ($NO_3^- + Cl^-$)

However, for the repository system, the thermal pulse may last for many years and there will be sufficient time for the unstable salt to decompose as long as the thermodynamics for the decomposition is favorable.

Figure 3-4 shows that the ratio of NO_3^- to Cl^- was high when the ratio of the nonvolatile cations ($Na^+ + K^+$) to the principal anions ($NO_3^- + Cl^-$) was low, suggesting that the vapor phase contained more nitric acid than hydrochloric acid. Figure 3-4 also indicates that the high ratio of NO_3^- to Cl^- in the condenser was not due to the high ratio of NO_3^- to Cl^- in the liquid phase (see Section 3.1.2).

3.1.2 Liquid Phase Chemistry

The analysis results for the samples taken from the liquid phase of the equimolar salt mixture at 150 and 180 °C [302 and 356 °F], are shown in Table 3-2. The volumes of the liquid salt mixture used in the calculation for concentration were the values at the test temperature; the concentrations given in Table 3-2 are the values at the test temperature. The ratios of NO_3^- to Cl^- were 20.9 at 150 °C [302 °F], and 16.4 at 180 °C [356 °F], respectively.

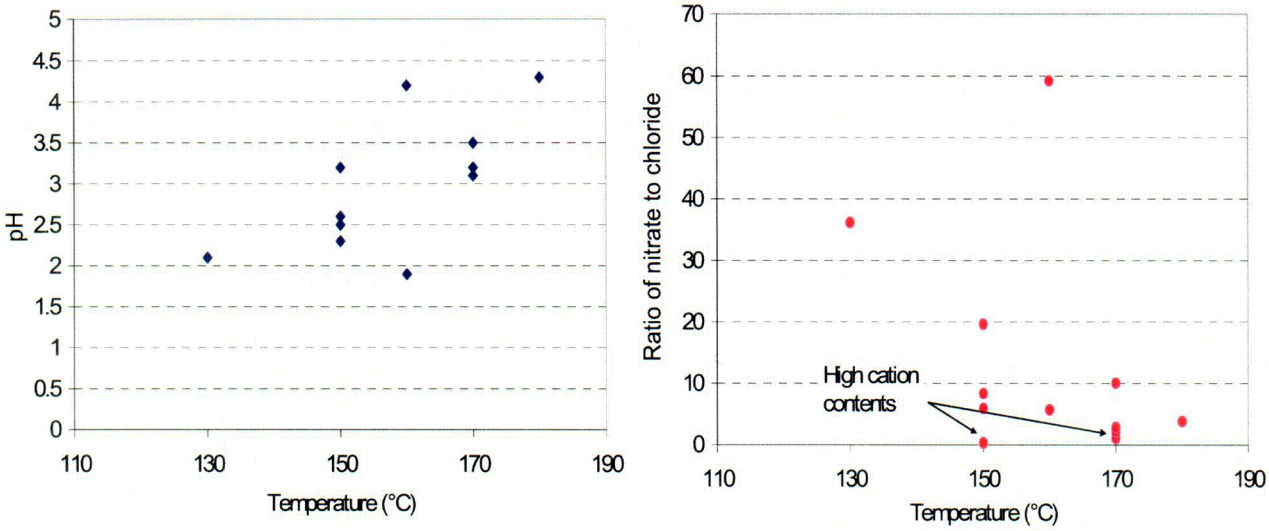

(a) (b)

Figure 3-2. (a) Measured pH and (b) Molar Ratio of Nitrate to Chloride in the Condensate As a Function of Temperature

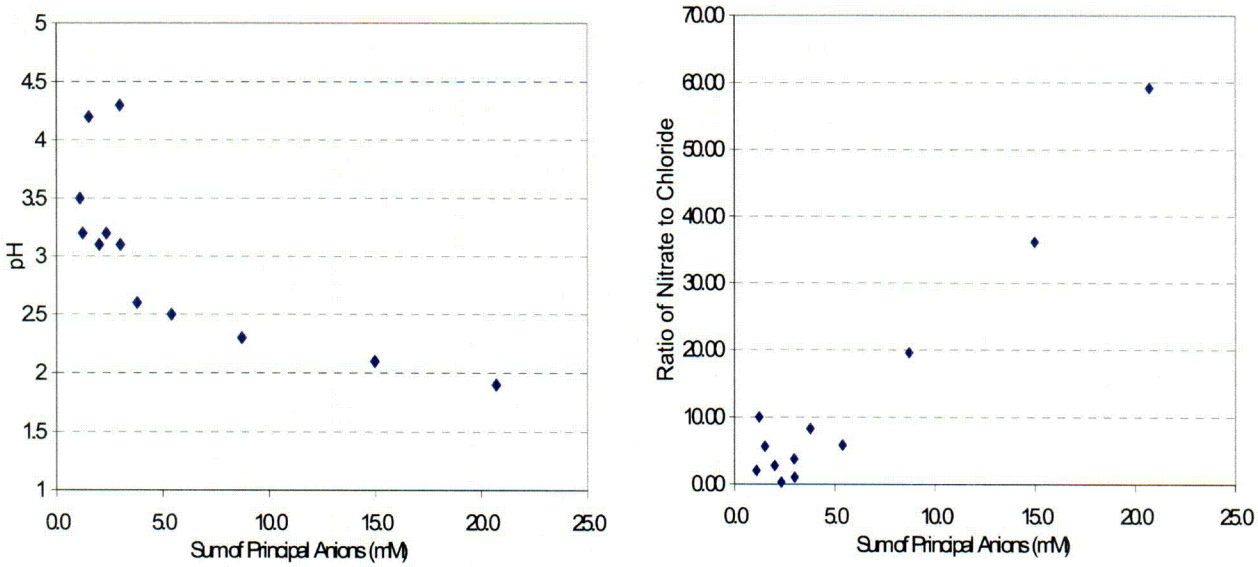

(a) (b)

Figure 3-3. (a) pH and (b) Ratio of Nitrate-to-Chloride of the Condensate As a Function of the Sum of the Principal Anions (NO_3^- + Cl^-)

C01A

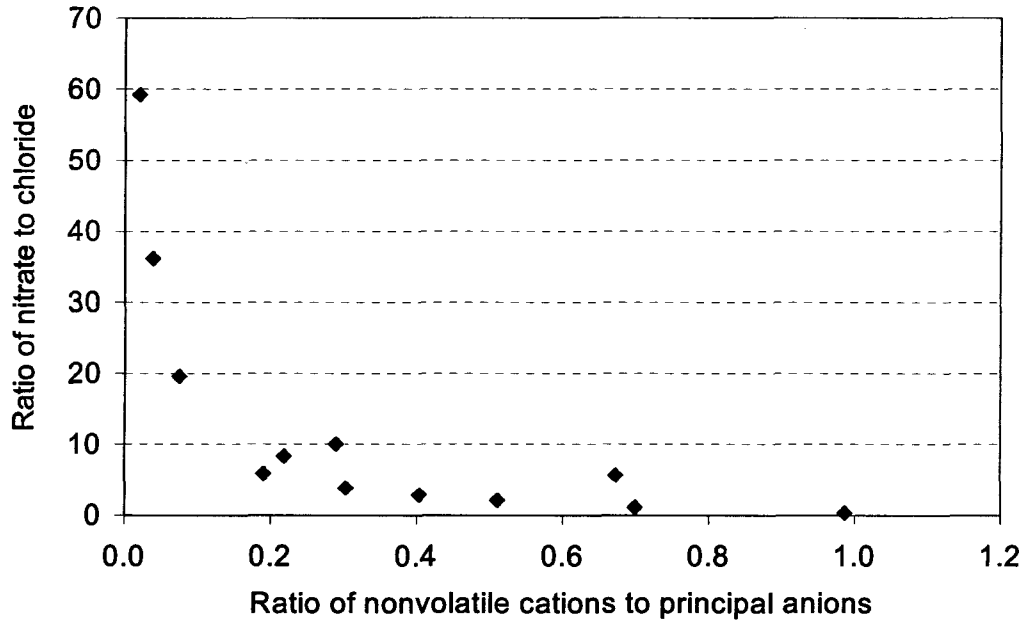

Figure 3-4. Ratio of Nitrate to Chloride As a Function of the Sum of Nonvolatile Cations ($Na^+ + K^+$) to the Sum of the Principal Anions ($NO_3^- + Cl^-$)

Table 3-2. Analyzed Liquid Phase Composition of the Salt Mixture at Test Temperatures*

Temperature (°C) [°F]	Volume (mL)*	Weight (g)†	Cl^- Concentration (M)	NO_3^- Concentration (M)	$[NO_3^-]/[Cl^-]$ Concentration Ratio
150 [302]	17	35.61	0.93	19.41	20.9
180 [356]	14.5	31.95	1.27	20.83	16.4

*Note: The volumes and concentrations are the values at the test temperatures.
†1 oz = 29.57 mL.
‡1 lb = 454 g.

3.2 Corrosion Behavior of Alloy 22 Materials

3.2.1 Open-Circuit Potential

Figure 3-5 shows the measured open-circuit potentials of the various Alloy 22 specimens (see Table 2-1) in solutions saturated with the equimolar $NaCl$-$NaNO_3$-KNO_3 salt mixture at 160 °C [320 °F]. The open-circuit potentials lay between 0.270 and 0.370 V_{SCE}, except for one creviced and welded plus solution annealed specimen whose potential was 0.170 V_{SCE} initially, but increased to 0.185 V_{SCE} after 1,000 seconds of immersion. It is not known why the open-circuit potential of this specimen was lower than those of the other specimens. No difference in the open-circuit potential was observed among the specimens with different metallurgical conditions.

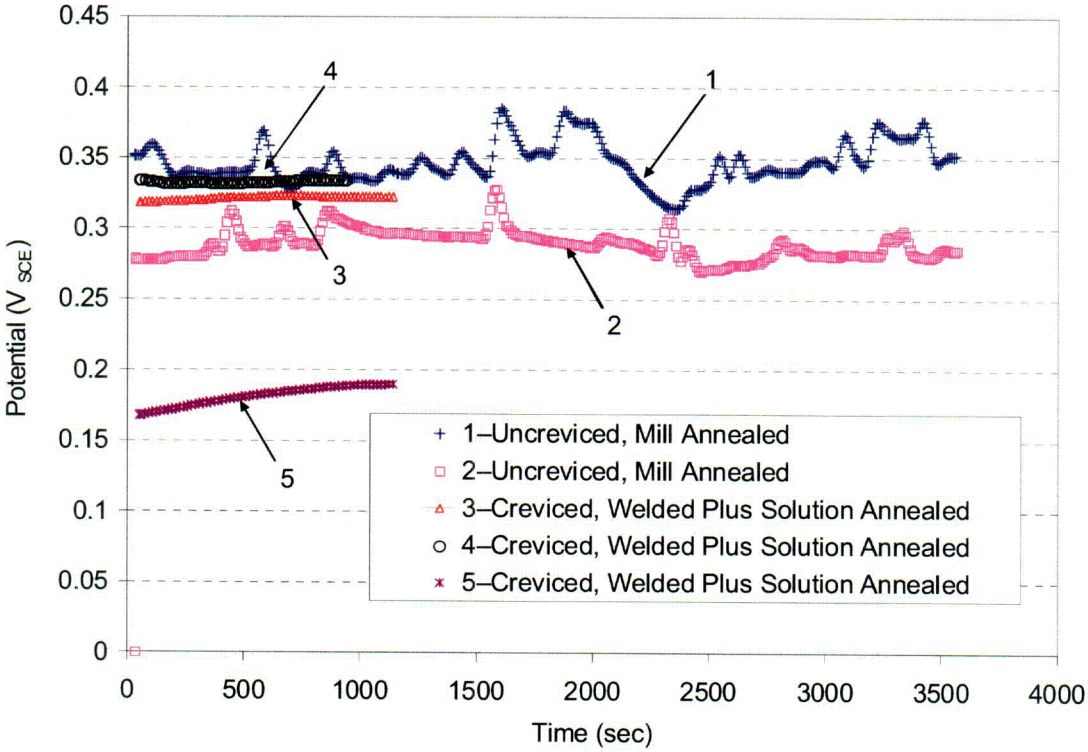

Figure 3-5. Open-Circuit Potentials of Alloy 22 Specimens in Concentrated $NaCl$-$NaNO_3$-KNO_3 Solutions at 160 °C [320 °F].
Note: Specimens 1 and 2 Were the *M.A. Cylinder*; Specimen 3 Was the *Creviced, Welded Plus Solution-Annealed-20*; and Specimens 4 and 5 Were the *Creviced, Welded Plus Solution-Annealed-240* Specimens in Table 2-1.

Figure 3-6 shows the open-circuit potentials of the Alloy 22 specimens (see Table 2-1) that were measured over a longer-term exposure (up to 100 hours), and the comparison with the oxidation and reduction potentials (also called ORPs) of the concentrated solution saturated with the equimolar $NaCl$-$NaNO_3$ -KNO_3 salt mixture at 160 °C [320 °F] measured on a platinum electrode. The stabilized open-circuit potentials of the Alloy 22 specimens were 200 to 300 mV lower than those measured on the platinum electrode. The closeness of the Alloy 22 open-circuit potentials to the platinum potential suggests that the Alloy 22 specimens did not undergo significant localized attack (Kolts and Sridhar, 1984), which was confirmed by the posttest surface examination. The high potential (close to 0.5 V_{SCE}) measured on the platinum electrode indicates that the system was oxidizing during the experiment.

3.2.2 Potentiodynamic Polarization Behavior

Figure 3-7 shows typical potentiodynamic polarization curves obtained with a creviced, welded plus solution annealed and an uncreviced mill-annealed specimens of Alloy 22. During the anodic potential scans from the open-circuit potentials, the current density increased rapidly to 1.1×10^{-6} to 3.0×10^{-6} A/cm^2 [7.1×10^{-6} to 1.9×10^{-5} A/in^2] within a few millivolts above the open-circuit potential. When the potential reached E_1 (400 to 550 mV_{SCE}), the corrosion current started to increase. On reversing the potential scan, the current density decreased to the previous values of i_1 at potential E_2 (490 to 600 mV_{SCE}). There was no significant hysteresis

C02

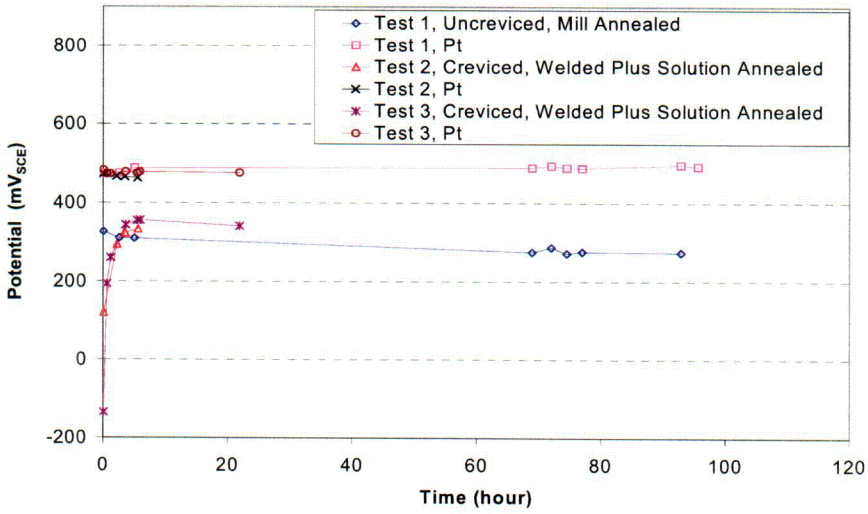

Figure 3-6. Comparison of the Oxidation-Reduction Potential Measured with a Platinum Electrode with the Open-Circuit Potentials of Alloy 22 Specimens in Concentrated NaCl-$NaNO_3$-KNO_3 Solutions at 160 °C [320 °F].
Note: The Mill-Annealed Specimen Was the *M.A. Cylinder*; and Creviced Specimens Were the *Creviced, Welded Plus Solution-Annealed-240* Specimens in Table 2-1.

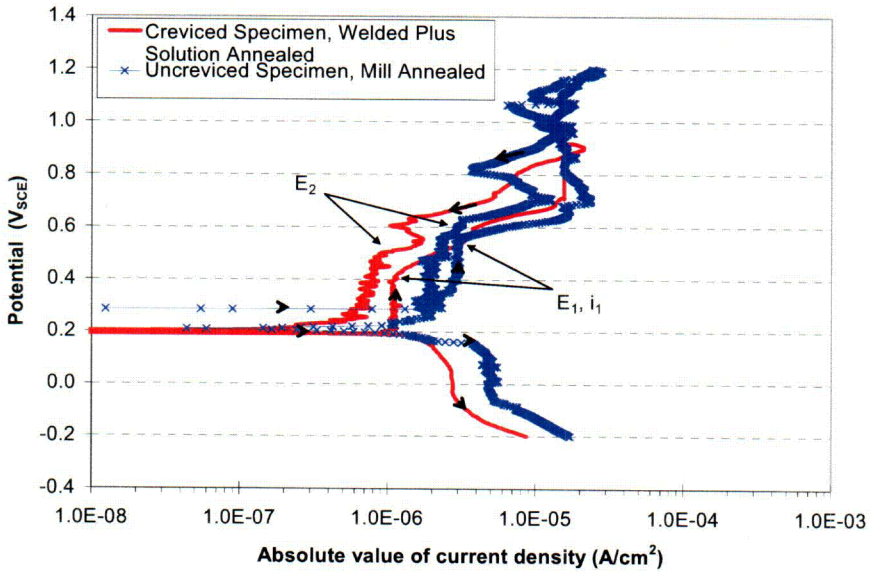

Figure 3-7. Potentiodynamic Polarization Curves on Alloy 22 Electrodes in Concentrated NaCl-$NaNO_3$-KNO_3 Solution at 160 °C [320 °F]. Potential Scan Rate: 0.167 mV/sec.
Note: 1 A/cm^2 = 6.45 A/in^2. The Mill-Annealed Specimen Was the *M.A. Cylinder*; and Creviced Specimens Were the *Creviced, Welded Plus Solution-Annealed-240* Specimens in Table 2-1.

C03

in the polarization curves. Therefore, the polarization curves suggest that there was no significant localized corrosion attack on the creviced or on the uncreviced Alloy 22 specimens. No sign of localized corrosion attack was observed under microscope after the specimens were removed from the test vessels either.

3.2.3 Vapor Phase and Liquid Phase Exposure Tests

Figure 3-8 shows the corrosion rate results calculated from weight loss of specimens exposed to the vapor and liquid phases. The metallurgical conditions of the specimens shown in Figure 3-8 include thermally aged, as-welded, and welded plus solution-annealed specimens. The specimens were either uncreviced or creviced. The tests were conducted in the temperature range from 150 to 180 °C [302 to 356 °F]. The test durations were from 32 to 80 days. The effects of liquid and vapor phases, temperature, crevice, metallurgical conditions, and exposure time are discussed in the following sections.

3.2.3.1 Corrosion of Alloy 22 in Vapor and Liquid Phases

As shown in Figure 3-8, the general corrosion rates based on weight loss ranged from 0.95 to 9.4 µm/yr [0.037 to 0.37 mils/yr] for the specimens exposed to the liquid phase, and from 0.17 to

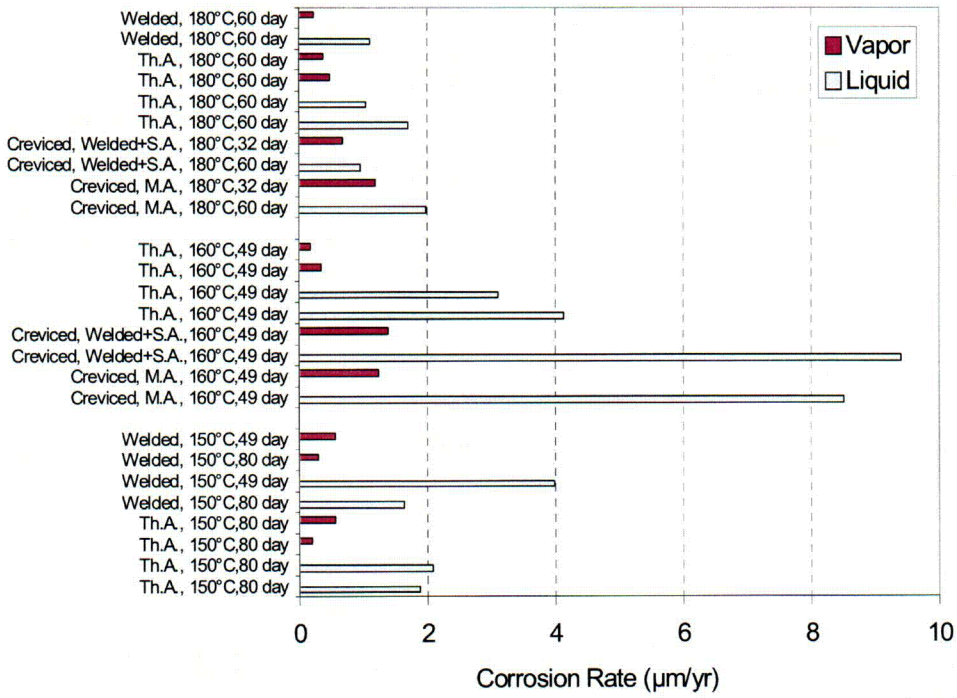

Figure 3-8. Corrosion Rate Calculated From Weight Loss of Specimens in the Vapor Phase and Liquid Phase Exposure Tests. Note: 1 mil = 25.4 µm. Th. A. Stands for *Th. A. Plate*; Welded Stands for *Welded Plate*; Crevice, Welded+S.A. Stands for *Creviced, Welded Plus Solution-Annealed-20*; and Creviced, M.A. Stands for *Creviced M.A.* in Table 2-1.

C04

1.37 μm/yr [0.0067 to 0.054 mils/yr] for the specimens exposed to the vapor phase. Hence, the specimens were significantly more corroded in the liquid phase than in the vapor phase. Figure 3-9 shows a comparison of the posttest appearances of a thermally aged specimen exposed partially to the liquid phase and partially to the vapor phase during the test. The liquid phase section was significantly corroded by general corrosion. The vapor phase section was slightly corroded and the polishing marks on the specimen in this section were clearly visible. The corrosion mode in the vapor phase was mainly grain boundary attack. The surface of the specimen shown in Figure 3-9 was vertically placed in the test vessel. However, the horizontally-placed surfaces of some of the Alloy 22 specimens exposed to the vapor phase were heavily corroded (Figure 3-10). In some areas, the attack was not uniform. The depth at the deepest corroded areas were approximately the same as those exposed to the liquid phase. Because these surface were placed horizontally, liquid condensate dripping from the top of the vessel might have collected on these surfaces during the test. This condensate was acidic and corrosive to the Alloy 22 specimens.

3.2.3.2 Effect of Temperature on the General Corrosion Rate of Alloy 22

Figure 3-11 is a rearrangement of Figure 3-8, showing the corrosion rates of only the uncreviced specimens in the vapor and liquid phases at 150, 160 and 180 °C [302, 320, and 356 °F]. It appears that the corrosion rate was lower at high temperatures than at low temperatures, which is contrary to the usual temperature dependence. As mentioned in Section 2.2, the temperatures of the liquid and vapor phases sometimes deviated from the set temperature by up to ± 25 °C [± 45 °F] during the evaporation of excess water. More temperature data obtained under the same condition and within the same exposure duration are required to understand temperature dependence of the corrosion rates.

(a) (b)

Figure 3-9. Corrosion of a Thermally Aged Alloy 22 Specimen (*Th. A. Plate* in Table 2-1) in Liquid and Vapor Phases After Exposure at 160 °C [320 °F]

C05

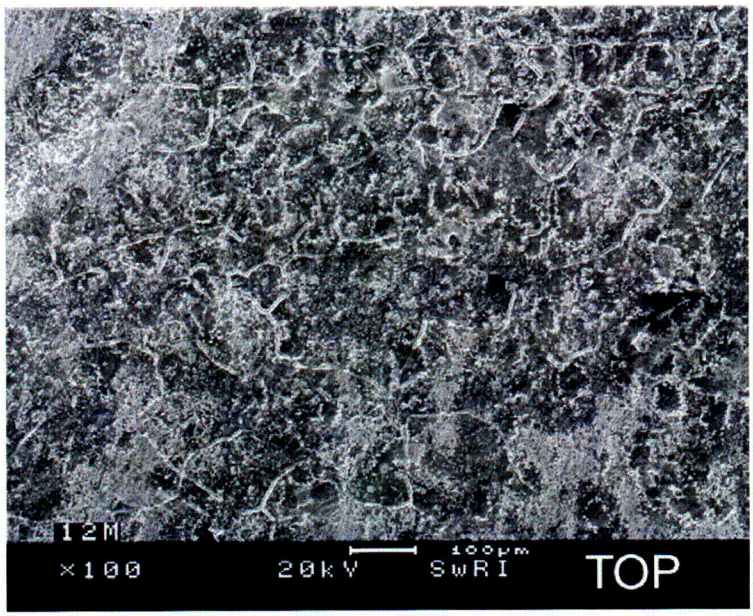

Figure 3-10. Corrosion of the Horizontal Surface of Alloy 22 Specimen (*Creviced, Welded Plus Solution-Annealed-20* in Table 2-1) in Vapor Phase After Exposure at 160 °C [320 °F]

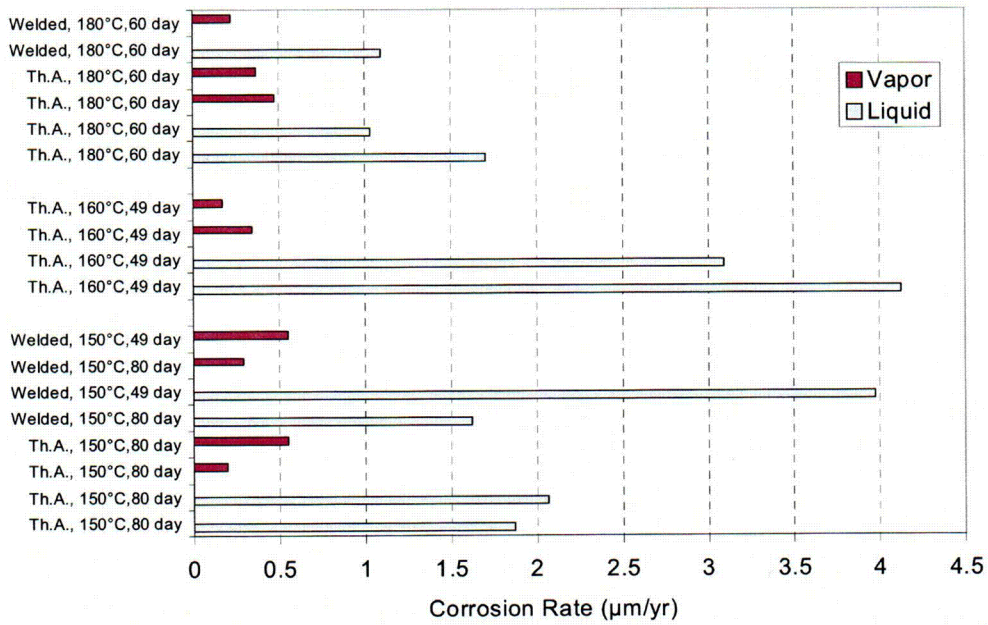

Figure 3-11. Corrosion Rates of Uncreviced Specimens at Three Different Temperatures As Shown in Figure 3-8.
Note: 1 mil = 25.4 µm. Th. A. Stands for *Th. A. Plate*, and Welded Stands for *Welded Plate* Specimens in Table 2-1.

COG

3.2.3.3 Effect of Crevice on Corrosion of Alloy 22

Figure 3-12 shows the effect of crevice on the corrosion of Alloy 22 specimen in Table 2-1. The uncreviced area was severely corroded by general corrosion, while the creviced area was only slightly corroded. Polishing marks were clearly visible in the creviced area, but not in the uncreviced area. No apparent localized corrosion was observed in the creviced area. However, some deep areas can be seen at the interface between the creviced area and the uncreviced area (dark areas in Figure 3-12b,c). Using the differential planar focusing method on a microscope, the depth in these areas was approximately the same as the depth of the uncreviced areas. Therefore, the primary attack mode for Alloy 22 appears to be by general corrosion in the $NaCl$-$NaNO_3$-KNO_3 salt mixture under the test conditions.

3.2.3.4 Effect of Welds on Corrosion of Alloy 22

Figure 3-13 shows the posttest optical appearance of a welded specimen in Table 2-1 exposed to the liquid phase and the scanning electron microscope picture at the interface between the weld and the base metal. After the liquid phase exposure, the microstructure of the welded area were clearly different from the base metal. The scanning electron microscope picture also shows that the corrosion in the welded area was along the dendritic structure.

3.2.3.5 Exposure Time Effect on the Corrosion Rate of Alloy 22

The corrosion rates shown in Figure 3-8 were grouped into the following four categories:

(1) Vapor phase corrosion rates of creviced specimens
(2) Vapor phase corrosion rates of uncreviced specimens
(3) Liquid phase corrosion rates of creviced specimens
(4) Liquid phase corrosion rates of uncreviced specimens

The general corrosion rates for these categories of specimens are plotted as a function of time, along with test temperature (Figure 3-14). In the liquid phase, the longer the exposure time, the lower the corrosion rate. This time dependence trend is similar to those reported by the DOE (Bechtel SAIC Company, LLC, 2003). In the vapor phase, the measured values were low and no significant time dependence was observed. As discussed in Section 3.2.3.2, the effect of temperature on the corrosion rate was not conclusive because the temperature deviated significantly from the set temperature when an excess amount of water was present during the test.

3.3 Comparison with DOE Work

The DOE also conducted limited experiments for the corrosion of Alloy 22 materials in highly concentrated salt solutions at elevated temperatures. The following presents the comparisons for the results obtained by the DOE with the results obtained in the present studies.

3.3.1 Open-Circuit Potential

The DOE conducted measurements for the open-circuit and repassivation potentials for Alloy 22 material in a pure nitrate salt (42 molal NO_3^-) and several concentrated nitrate-chloride salt

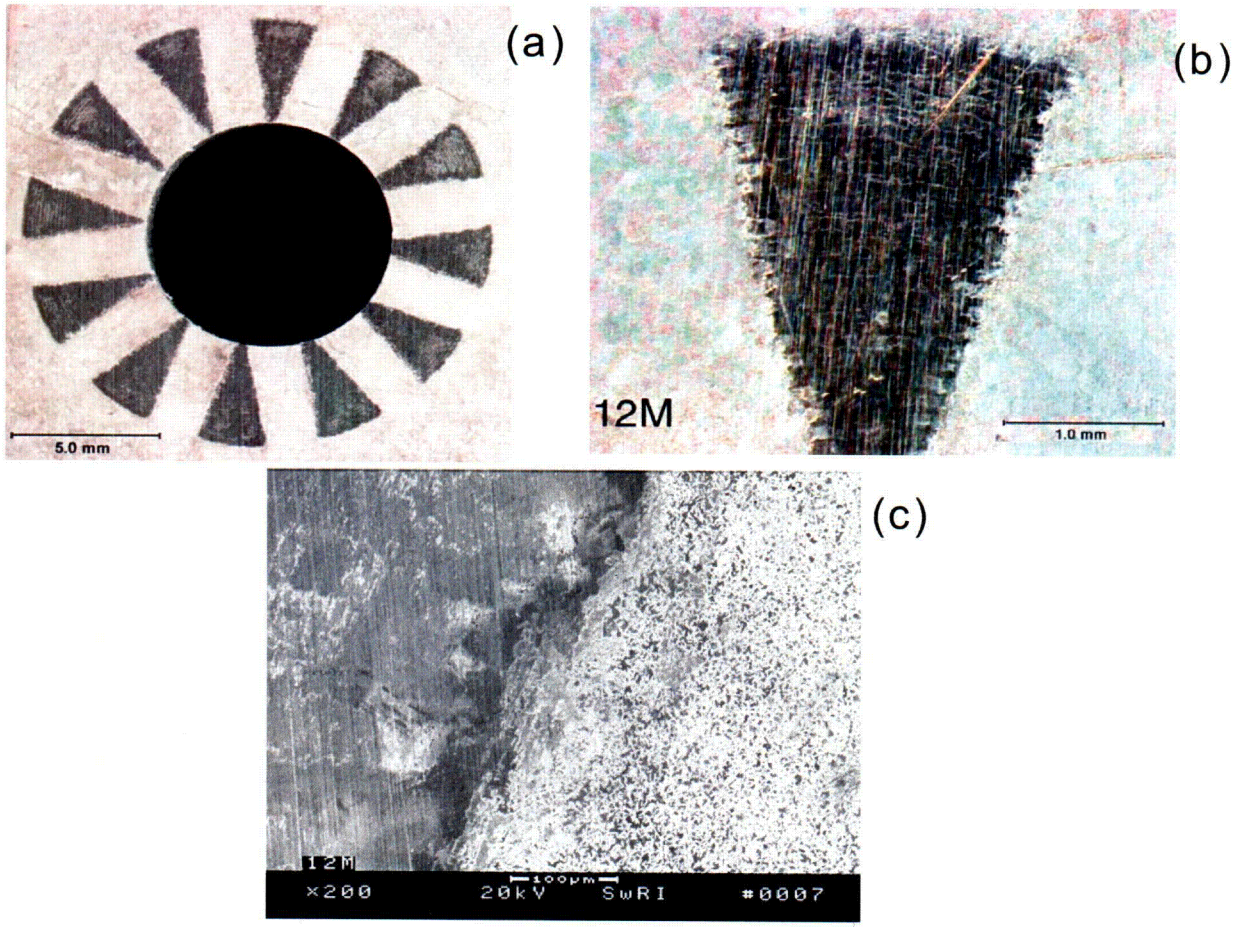

Figure 3-12. (a) Corrosion of a Partially Creviced Specimen, (b) Corrosion Near a Creviced Area, and (c) Corrosion at the Interface Between a Creviced Area and an Uncreviced Area. The Uncreviced Area Were Actively Corroded and the Creviced Area Were Only Slightly Corroded After Exposure at 160 °C [320 °F].
Note: The Specimen Was a *Creviced, Welded Plus Solution-Annealed-20* Specimen in Table 2-1. The Darker Areas Were the Creviced Areas. Pronounced Nonuniform Attach Formed at the Interface Between the Creviced and Uncreviced Area.

C07

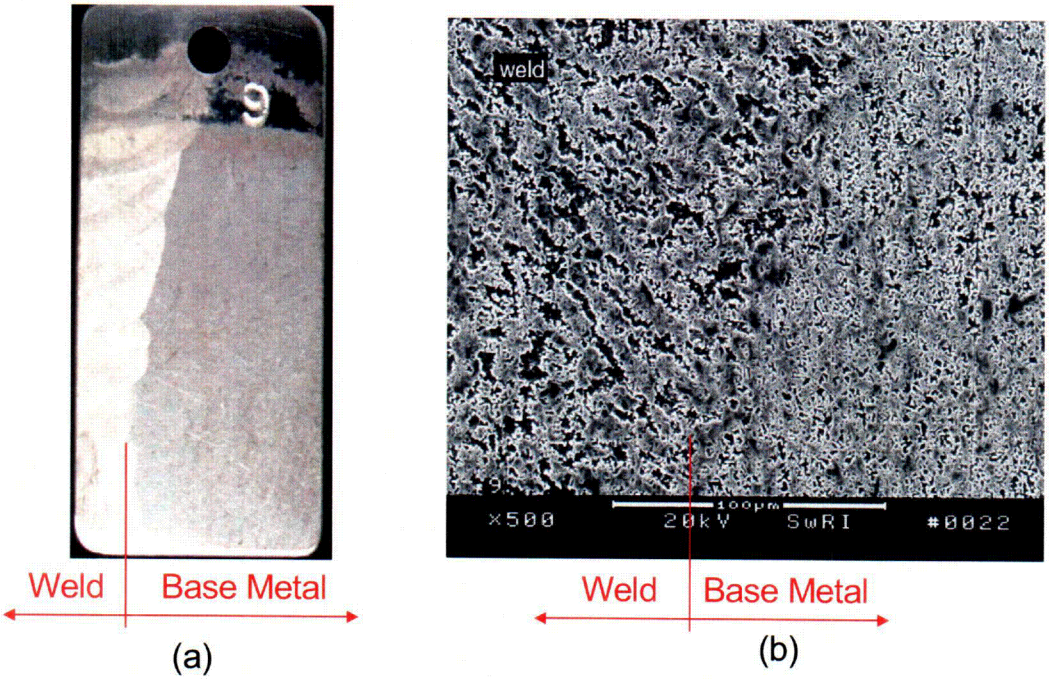

Figure 3-13. Optical and Scanning Electron Microscope Pictures Showing the Corrosion of a Welded Specimen Near the Weld After Exposure at 160 °C [320 °F].
Note: The Specimen Was a *Welded Plate* Specimen in Table 2-1.

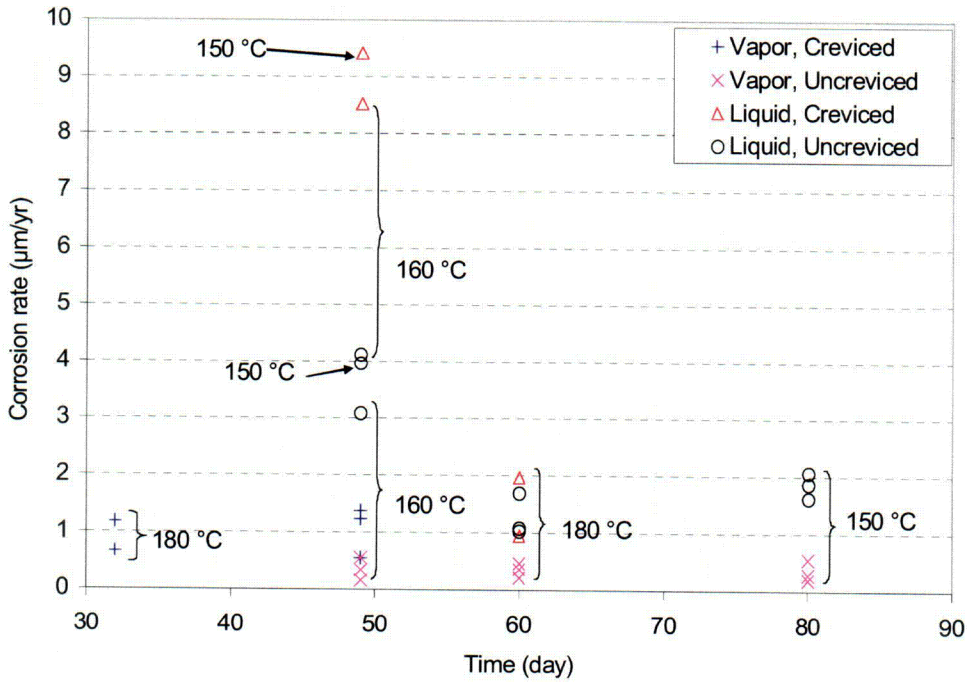

Figure 3-14. General Corrosion Rates As a Function of Exposure Time for the Data Shown in Figure 3-8

C08

mixtures in deaerated systems at ambient pressure.[2] Figure 3-15 shows the comparison between the open-circuit potentials reported by the DOE and the values presented in Figure 3-6. Because the open-circuit potentials presented by the DOE were after 24 hours immersion, only those data that were obtained at or beyond 24-hour exposure time in Figure 3-6 were used for comparison in Figure 3-15. The concentration of the anions used in the present work was close to 0.93 M Cl^- and 19.4 M NO_3^-, the saturated solution by the equimolar NaCl-$NaNO_3$-KNO_3 mixture at 150 °C [302 °F] (Table 3-2). It is not known if the concentrations of the solutions reported in the DOE tests were the values calculated based on the amount of salt added or measured at the actual temperature. If the concentrations were calculated based on the initial addition of the salts, the actual values for some of the mixtures might be lower than the values indicated in Figure 3-15 because of the solubility limit at the given temperatures. In general, the results reported by the DOE were approximately -0.35 V versus a saturated silver-silver chloride electrode and the results from the present work measured in the system that was not deaerated were approximately 0.3 V versus a saturated calomel electrode. At 25 °C [77 °F], the difference between the potential of a silver-silver chloride electrode and the potential of a saturated calomel electrode is 0.045 V (the silver-silver chloride has a lower potential) (Bard and Faulkner, 1980). Therefore, the open-circuit potentials measured by DOE is approximately -0.395 V versus the saturated calomel electrode. It is not known what kind of salt bridge was used by DOE. If the difference between the thermal liquid junction potentials of the two reference electrodes could be ignored, the open-circuit potentials measured by DOE in deaerated closed system were more than 0.6 V lower than the potentials obtained in the present study, which were carried out in a system that was not deaerated at ambient pressure. The reported difference between the repassivation potentials and the open-circuit potentials measured in the deaerated closed system were 0.95 to 1.2 V.[3] For the evaluation of the susceptibility of Alloy 22 to localized corrosion under the potential repository environments, the open-circuit potentials measured in a system that is not deaerated should be used because the potential repository will be exposed to the atmosphere. The difference between the repassivation potentials (which should be independent of deaeration) and the open-circuit potentials that are more realistic under the Yucca Mountain conditions is 0.35 to 0.6 V, which is still an indicator of no localized corrosion, but 0.6 V less than the values used by the DOE.

3.3.2 Weight Loss Measurements

The DOE has an on-going program to test the corrosion rates of Alloy 22 foil specimens in nitrate-chloride mixtures at elevated temperatures (Orme, et al., 2004). The test conditions that are relevant to the present study are the 4-month weight loss measurements for Alloy 22 specimens in the liquid and vapor phases of a closed pressurized system containing 21.2 molal of salt mixture (NO_3^-/Cl^- = 6.7).

Figure 3-16 shows the comparison between the corrosion rates of Alloy 22 specimens in the concentrated nitrate-chloride salt mixtures measured by the DOE in closed autoclave systems and those measured in the present work in the systems that were not deaerated. The negative

---

[2]Ilevbare, G. "Effect of Dust Deliquescence on Localized Corrosion of Waste Package Outer Barrier (Alloy 22)." Presentation at the Nuclear Waste Technical Review Board, November 8–9, 2005. Slides 8–12. Las Vegas, Nevada. 2005.

[3]Ibid.

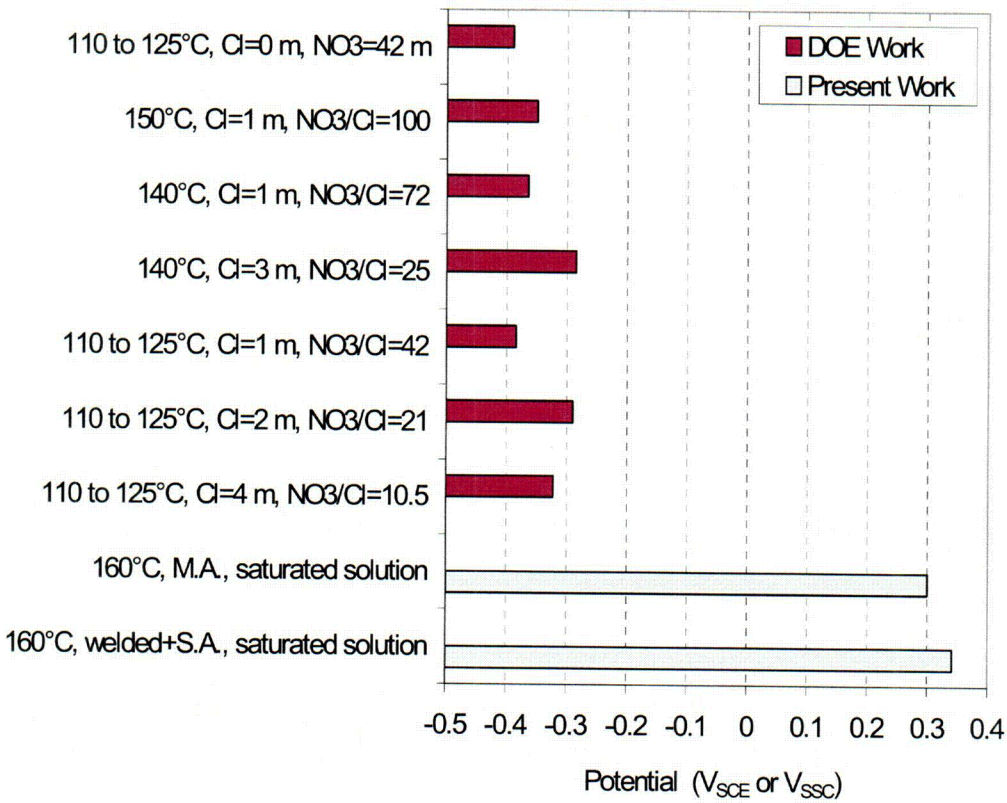

Figure 3-15. Steady-State Open-Circuit Potentials Measured by DOE in Deaerated Solutions Against Saturated Silver-Silver Chloride Electrode[4] and Measured in the Present Work Against Saturated Calomel Electrode As Shown in Figure 3-6. Note: $V_{SCE} - V_{SSC}$ = 0.045 V if the Thermal Liquid Junction Potential Is Ignored at 25 Percent. Cl = Chloride, NO3 = Nitrate, NO3/Cl = Nitrate-to-Chloride Ratio.

[4]Ilevbare, G. "Effect of Dust Deliquescence on Localized Corrosion of Waste Package Outer Barrier (Alloy 22)." Presentation at the Nuclear Waste Technical Review Board, November 8–9, 2005. Slides 8–12. Las Vegas, Nevada. 2005.

C09

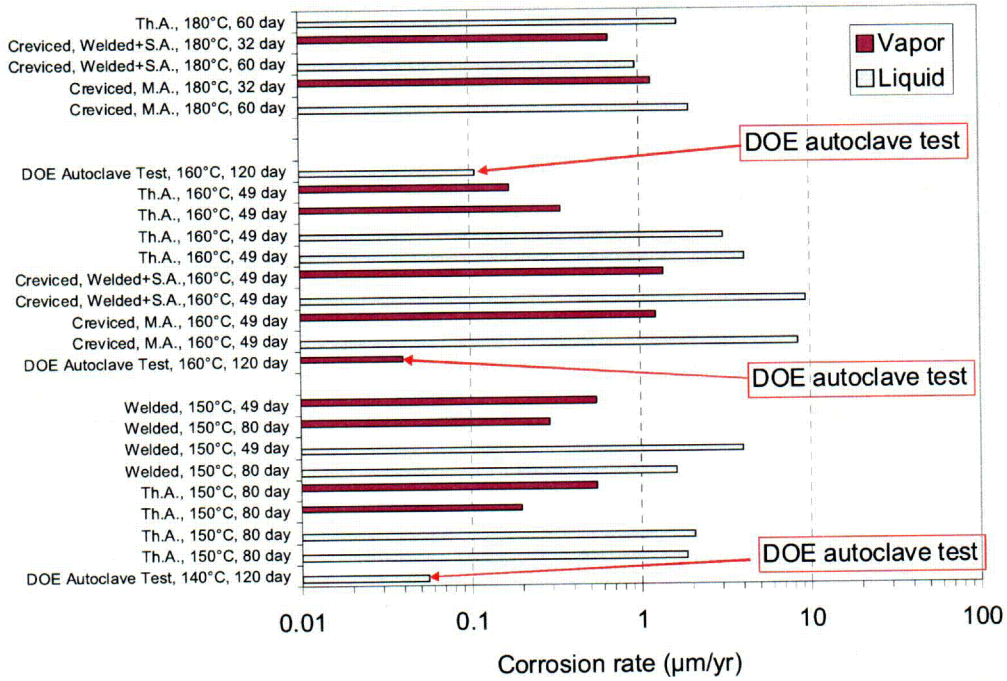

Figure 3-16. Comparison Between the Corrosion Rates of Alloy 22 Specimens in Concentrated Nitrate-Chloride Salt Mixtures Measured by DOE in the Closed Autoclave Systems (Orme, et al., 2004, Tables 3 and 4, and Figure 6. Note that Table 3 Indicates that the Test Period Was 4 Months, But Figure 6 Seems to Indicate that the Test Period Was 160 Days.) and Measured in the Present Work in the System that Was Not Deaerated As Shown in Figure 3-8.

corrosion rates reported by the DOE were not included in Figure 3-16. In both the liquid phase and the vapor phase tests, the DOE weight loss results were 10 to 50 times lower than those measured in the present work. This large difference was probably due to the low partial pressure (or fugacity) of oxygen in the closed pressurized autoclave system used in the DOE tests. The low corrosion rates obtained by the DOE is consistent with the open-circuit potential measurements as discussed in Sections 3.2.1 and 3.3.1; the open-circuit potentials of Alloy 22 in the deaerated system were much lower than those measured in the system that was not deaerated, even though nitrate is a highly oxidizing agent. The low open-circuit potentials in closed system were probably the cause of the low corrosion rate measured in the DOE tests because corrosion rate varies with the oxidation/reduction conditions in the environment.

The large difference between the low corrosion rates measured by the DOE and the high corrosion rates measured in the present study may also be partly due to (i) the exposure time effect as discussed in Section 3.2.3.4, or (ii) the differences in metallurgical treatment conditions. The DOE tests were conducted in a 4-month duration with thin foil specimens and the tests in present work were conducted between 32 to 80 days, with the majority of the specimens being thermally aged at 870 °C [1,598 °F] for 30 minutes. It is not known how the foil specimens used in the DOE tests were metallurgically treated. It has been reported that

C10

thermally aged Alloy 22 specimens had a lower resistance to both localized and general corrosion (Dunn, et al., 2003). Thermally aging at 870 °C [1,598 °F] simulates the welding effect in the heat-affected zone of the Alloy 22 waste package container. Therefore, the corrosion rate measured with thermally aged specimens may represent the worst-case corrosion rates for Alloy 22 containers.

Similar corrosion rate measurements for Alloy 22 material were conducted by Pulvirenti, et al. (2003, 2004) in concentrated brine solutions containing Mg^{2+}, Ca^{2+}, Na^{+}, K^{+}, Cl^{-}, and NO_3^{-}. Because of the hydrolysis of the alkaline earth metals, Cl_2, NO, NO_2, HCl, and HNO_3 were detected in the vapor phase of the system during evaporation. The pH of the vapor condensate and the residual liquid were found to be close to 1 or less. The corrosion rates of Alloy 22 were found to be on the order of 5 to100 µm/yr [0.2 to 4 mils/yr] over the temperature range of 110 to 145 °C [230 to 293 °F]. Pitting corrosion was also observed in some of the specimens. No heat treatment was mentioned in the publications by Pulvirenti, et al. (2004); the specimens used in these tests were likely mill-annealed.

The corrosion rate of Alloy 22 below or at the boiling temperatures {slightly over 100 °C [212 °F]} have been reported by the manufacturers of the alloy for a wide range of chemical solutions. According to Haynes International,[5] the corrosion rate of Alloy 22 in dilute nitric acid (10 wt%) at temperatures up to the boiling temperature is relatively low {<25 µm/yr [1 mil/yr]}. However, the general corrosion rate of Alloy 22 in hydrochloric solutions varies from 75 to 10,000 µm/yr [3 to 400 mils/yr] when the concentration changes from 1 to 10 wt% at boiling temperatures. In a mixture containing 4.9 wt% HNO_3 and 0.125 wt% HCl, the corrosion rate of Alloy 22 was 50 µm/yr [2 mils/yr] at boiling temperature.

The corrosion rates measured in the evaporative $NaCl$-$NaNO_3$-KNO_3 solution {1 to 10 µm/yr [0.04 to 0.4 mils/yr]} indicate that the corrosivity of the Na^{+}-K^{+}-NO_3^{-}-Cl^{-} system is close to that of the Ca^{++}-Mg^{++}-Na^{+}-K^{+}-NO_3^{-}-Cl^{-} system, but significantly lower than those of the boiling hydrochloric acid or the mixture of nitric and hydrochloric acid.

[5]Haynes International. "HASTELLOY C-22 Alloy." Bulletin H–2019F. 2002.

4 SUMMARY, CONCLUSIONS, AND RECOMMENDATIONS

4.1 Chemistry of Nitrate-Chloride Mixtures

The chemistry of the equimolar $NaCl$-$NaNO_3$-KNO_3 salt mixtures were studied in the temperature range of 130 to 180 °C [266 to 356 °F] at ambient pressure in a system that was vented to the open air. The vapor phase composition was evaluated by the water samples collected from a condenser. The pH of the vapor phase condensate was found to be as low as 2, which suggests that the salt mixture containing only monovalent alkaline metals of nitrates and chlorides was not thermodynamically stable and decomposed slowly to form acid gases. The chemical composition measurements of the condensates showed that nitric acid was the primary acidic components. The concentration ratio of nitric acid to hydrochloric acid was high (2 to 59.2) for the samples that were not significantly contaminated by the liquid phase components. The higher content of nitric acid than hydrochloric acid in the vapor phase implies that in the deliquescent dusts that may be deposited onto the waste package and drip shield surfaces, nitrates may decompose preferentially to the chlorides during the thermal pulse period. Therefore, the ability of inhibiting localized corrosion of Alloy 22 by the nitrates may be compromised.

4.2 Electrochemical Behavior of Alloy 22

The open-circuit potentials of Alloy 22 specimens with different metallurgical conditions (mill annealed, welded plus solution annealed) were measured in a system that simulates the potential repository environments. Because of the presence of air in the system that was not deaerated, the stabilized open-circuit potential was 0.3 V_{SCE}. The U.S. Department of Energy (DOE) also conducted measurements for the open-circuit potentials of Alloy 22 material in similar salt mixtures in deaerated systems at ambient pressure. In the deaerated system, the measured open-circuit potential was approximately −0.395 V_{SCE}. If the difference between the thermal liquid junction potentials in the DOE tests and in the present work is ignored, the open-circuit potential measured by DOE in deaerated closed systems was more than 600 mV lower than the potential obtained in the present study which was carried out in an ambient-pressure system that was not deaerated. For the evaluation of the susceptibility of Alloy 22 to localized corrosion under the potential repository environments, the open-circuit potential values measured in the system that is not deaerated should be used because the potential repository will be exposed to the atmosphere.

Potentiodynamic polarization behavior of Alloy 22 were also measured with both uncreviced and creviced specimens. The polarization curves showed no significant sign of localized corrosion.

4.3 Corrosion Rate

Creviced and uncreviced Alloy 22 specimens were exposed to both the vapor and the liquid phases of ambient pressure systems containing an equimolar $NaCl$-$NaNO_3$-KNO_3 salt mixture in the temperature range between 150 and 180 °C [302 and 356 °F] at ambient pressure. The results indicated no significant localized corrosion and general corrosion was found to be the primary attack mode. Compared with the general corrosion rates of Alloy 22 foil specimens in a similar salt mixture that were measured by DOE in closed autoclave systems, the corrosion rates from the present study were 10 to 50 times higher than those measured by DOE in closed

autoclave systems, in both the liquid phase and in the vapor phase. This large difference was probably due to the differences in the partial pressure of oxygen in the closed autoclave system used in the DOE tests and in the systems used in the present work. The large difference may also be due to the difference in initial metallurgical conditions. The majority of the test specimens used in the present weight loss study were thermally aged at 870 °C [1,598 °F] for 30 minutes. It is not known how the specimens used by the DOE were treated.

5 FUTURE WORK

The results presented in this report are preliminary and cover only the temperature range from 130 to 180 °C [266 to 356 °F]. Because of the recently reported higher boiling temperature {220 °C [428 °F]} for the $NaCl$-$NaNO_3$-KNO_3 salt mixtures, additional tests were planned for higher temperatures. Duplicate specimens with different metallurgical treatments (including mill-annealing, thermally aging at 870 °C [1,598 °F] for 30 minutes, and welding) will be used, and these tests will be conducted for a longer term (four to five months) to reduce the time effect. The work is in progress in the following areas.

5.1 Dust Effect on Corrosion of Alloy 22

The high corrosion rate presented in this study was measured in extremely large amount of salts relative to the surface area of the waste package, compared to the small amount of salt that may be deposited on waste packages in the potential repository. In addition, the nitrate and chloride salt mixtures under the potential repository conditions will be mixed with a relatively large amount of insoluble dusts. The corrosion of Alloy 22 by the soluble salt mixture in the presence of large amount of insoluble dust is expected to be reduced because the capillarity of the dust may reduce the ability of the soluble salt to contact with the waste package surfaces. The dust effect on corrosion of Alloy 22 has been planned in the future work.

5.2 Verification of Preferential Decomposition of Nitrate

The preferential decomposition of nitrates over chlorides may decrease the inhibiting ability to localized corrosion of Alloy 22 by nitrates. This phenomenon could have important implications in the prediction of the performance of waste packages. Therefore, more experiments are required to verify that if the observed decomposition behaviors of nitrate and chloride would continue as a function of time in a longer term test.

5.3 Passivity and Pitting Corrosion of Alloy 22

Although the nonuniformly corroded areas observed at the interface between the crevice and the uncreviced regions of the Alloy 22 specimens in the liquid phase and on the horizontal surfaces of some specimens in the vapor phase cannot be characterized as typical pitting corrosion, the depth of the deeper areas was close to the open areas attacked by general corrosion. Because the results were obtained in short terms, the specimens from the longer term test will be evaluated for the susceptibility of Alloy 22 to pitting corrosion in the highly concentrated nitrate-chloride salt mixtures.

6 REFERENCES

Agarwal, D.C. and W.R. Herda. "The 'C' Family of Ni-Cr-No Alloys' Partnership with the Chemical Process Industry: The Last 70 Years." *Materials and Corrosion*. Vol. 48. pp. 542–548. 1997.

Anderson, M.J., N.R. Brown, J.D. Cloud, P.R.Z. Russell, and J. Trautner. "Waste Package Design for License Application." Proceedings of the 10th International High-Level Radioactive Waste Management Conference, Las Vegas, Nevada, March 30–April 3, 2003. Section E–7. Published on CD-ROM. La Grange Park, Illinois: American Nuclear Society. pp. 714–720. 2003.

ASTM International. "Standard Practice for Preparing, Cleaning, and Evaluating Corrosion Test Specimens." G1–03 (Reapproved 2003). West Conshohocken, Pennsylvania: ASTM International. 2005.

Bard, A.J. and L.R. Faulkner. *Electrochemical Methods*. New York City, New York: John Wiley and Sons. 1980.

Bechtel SAIC Company, LLC. "WAPDEG Analysis of Waste Package and Drip Shield Degradation." ANL–EBS–PA–000001. Rev. 02. Las Vegas, Nevada: Bechtel SAIC Company, LLC. 2004a.

———. "Multiscale Thermohydrologic Model." ANL–EBS–MD–000049. Rev 02. Las Vegas, Nevada: Bechtel SAIC Company, LLC. 2004b.

———. "Technical Basis Document No. 6: Waste Package and Drip Shield Corrosion." Rev. 1. Las Vegas, Nevada: Bechtel SAIC Company, LLC. 2003.

Brossia, C.S., L. Browning, D.S. Dunn, O.C. Moghissi, O. Pensado, and L. Yang. "Effect of Environment on the Corrosion of Waste Package and Drip Shield Materials." CNWRA 2001-003. San Antonio, Texas: CNWRA. 2001.

Craig, L., S. Carrol, and T. Wolery. "Deliquescence of $NaCl$-$NaNO_3$ and KNO_3-$NaNO_3$ Salt Mixtures at 90 °C in Water-Rock Interaction." Wanty and Seal II, eds. Vol. 2. London, England: Taylor Francis Group. pp. 1,275–1,278. 2004.

Dunn, D.S., D. Daruwalla, and Y.-M. Pan. "Effect of Fabrication Processes on Material Stability–Characterization and Corrosion." CNWRA 2004-01. San Antonio, Texas: CNWRA. 2003.

Dunn, D.S., O. Pensado, Y.-M. Pan, R.T. Pabalan, L. Yang, X. He, and K.T. Chiang. "Passive and Localized Corrosion of Alloy 22—Modeling and Experiments." CNWRA 2005-02. San Antonio, Texas: CNWRA. 2005.

Dunn, D.S., L. Yang, C. Wu, and G.A. Cragnolino. "Effect of Inhibiting Oxyanions on the Localized Corrosion Susceptibility of Waste Package Container Materials." Proceedings of the Materials Research Society Conference: Scientific Basis for Nuclear Waste Management XXVIII, San Francisco, California, April 13–16, 2004. Symposium Proceedings 824. J.M. Hanchar, S. Stroes-Gascoyne, and L. Browning, eds. Warrendale, Pennsylvania: Materials Research Society. pp. 33–38. 2004.

Hailey, P. and G. Gdowski. "Thermogravimetric Thin Aqueous Film Corrosion Studies of Alloy 22: Calcium Chloride Solutions at 150 °C and Atmospheric Pressure." Proceedings of the Materials Research Society Conference. Symposium Proceedings 757. Pittsburgh, Pennsylvania: Materials Research Society. pp. 765-770. 2003.

Kolts J. and N. Sridhar. "Temperature Effect in Localized corrosion in Corrosion of Nickel Base Alloys." Proceedings of the International Conference on Corrosion of Nickel-Base Alloys." R.C. Scarberry, ed. Materials Park, Ohio: American Society for Metals. pp. 191–198. 1984.

Lvov S.N. and D.D. Macdonald. "Estimation of the Thermal Liquid Junction Potential of an External Pressure Balanced Reference Electrode." *Journal of Electroanalytical Chemistry.* Vol. 403. pp. 25–30. 1996.

National Atmospheric Deposition Program (NRSP–3)/National Trends Network. 2004. <http://nadp.sws.uiuc.edu> (May 17, 2004).

NRC. "Risk Insights Baseline Report." Rev. 00. Washington, DC: NRC. April 2004.

Orme, C.A., J. Gray, J. Hayes, L. Wong, R. Rebak, S. Carroll, J. Harper, and G. Gdowski. "Fiscal Year 2004 Summary Report: General Corrosion and Passive Film Stability." UCRL–TR–208588. Livermore, California: Lawrence Livermore National Laboratory. 2004.

Pabalan, R.T., L. Yang, and L. Browning. "Deliquescence Behavior of Multicomponent Salts: Effects on the Drip Shield and Waste Package Chemical Environment at the Proposed Nuclear Waste Repository at Yucca Mountain, Nevada." Scientific Basis for Nuclear Waste Management XXV. Symposium Proceedings 713. B.P. McGrail and G.A. Cragnolino, eds. Pittsburgh, Pennsylvania: Materials Research Society. pp. 37–44. 2002.

Pulvirenti, A., K. Needham, M. Adel-Hadadi, E. Bishop, A. Barkatt, C.R. Marks, and J.A. Gorman. "Corrosion Behavior of Alloy 22 under Conditions of Dynamic Groundwater Composition." Proceedings of the CORROSION 2003 Conference. Paper No. 693. Houston, Texas: NACE International. 2003.

Pulvirenti, A., K. Needham, M. Adel-Hadadi, and A. Barkatt, C. Marks, and J. Gorman. "Multi-Phase Corrosion of Engineered Barrier Materials." Proceedings of the CORROSION 2004 Conference. Paper No. 694. Houston, Texas: NACE International. 2004.

Rard, J. A. "Results from Boiling Temperature Measurements for Saturated Solutions in the Systems NaCl + KNO_3 + H_2O, $NaNO_3$ + KNO_3 + H_2O and NaCl + $NaNO_3$ + KNO_3 + H_2O." UCRL–TR–207054. Livermore, California: Lawrence Livermore National Laboratory. 2004.

Yang, L. "A Bare Metal Reference Electrode for Application in the High-Temperature and High-Pressure Coolants of Nuclear Reactors." Proceedings of the CORROSION '99 Conference. Paper No. 460. Houston, Texas: NACE International. 1999.

Yang, L., R.T. Pabalan, L. Browning, and D.S. Dunn. "Corrosion Behavior of Carbon Steel and Stainless Steel Materials under Salt Deposits in Simulated Dry Repository Environments." Scientific Basis for Nuclear Waste Management XXVII. Symposium Proceedings 757. R.J. Finch and D. B. Bullen, eds. Pittsburgh, Pennsylvania: Materials Research Society. pp. 791–797. 2003.

CNWRA 2006-02

CORROSION OF ALLOY 22 IN CONCENTRATED NITRATE AND CHLORIDE SALT ENVIRONMENTS AT ELEVATED TEMPERATURES— PROGRESS REPORT